

Position: Don't be Afraid of Over-Smoothing And Over-Squashing

Niklas Kormann¹ Benjamin Doerr¹ Johannes F. Lutzeyer¹

Abstract

Over-smoothing and over-squashing have been extensively studied in the literature on Graph Neural Networks (GNNs) over the past years. We challenge this prevailing focus in GNN research, arguing that these phenomena are less critical for practical applications than assumed. We suggest that performance decreases often stem from uninformative receptive fields rather than over-smoothing. We support this position with extensive experiments on several standard benchmark datasets, demonstrating that accuracy and over-smoothing are mostly uncorrelated and that optimal model depths remain small even with mitigation techniques, thus highlighting the negligible role of over-smoothing. Similarly, we challenge that over-squashing is always detrimental in practical applications. Instead, we posit that the distribution of relevant information over the graph frequently factorises and is often localised within a small k -hop neighbourhood, questioning the necessity of jointly observing entire receptive fields or engaging in an extensive search for long-range interactions. The results of our experiments show that architectural interventions designed to mitigate over-squashing fail to yield significant performance gains. This position paper advocates for a paradigm shift in theoretical research, urging a diligent analysis of learning tasks and datasets using statistics that measure the underlying distribution of label-relevant information to better understand their localisation and factorisation.

1. Introduction

A graph is a versatile data structure that is well-suited for describing complex systems, offering a mathematical foundation to analyse real-world systems using Graph Neural Networks (GNN). Gilmer et al. (2017) introduced the Mes-

¹Laboratoire d'informatique, CNRS, École polytechnique, Institut Polytechnique de Paris, Palaiseau, France. Correspondence to: Niklas Kormann <niklas.kormann@polytechnique.edu>.

sage Passing Neural Network (MPNN) framework in 2017, which serves as the foundation for most modern GNNs, with powerful variants like Graph Convolutional Networks (GCNs) (Kipf & Welling, 2017) and Graph Attention Networks (GATs) (Veličković et al., 2018; Brody et al., 2022) achieving state-of-the-art results on many graph learning tasks. These advances have spurred a wide range of applications. For example, GNNs are now routinely applied in chemistry and drug discovery for molecular property prediction (Li et al., 2021), in large-scale recommendation engines in social networks (Ying et al., 2018; Zhao et al., 2025; Liu et al., 2024), and in spatial-temporal forecasting for traffic prediction like for Google Maps (Yu et al., 2017; Derrow-Pinion et al., 2021). Theoretical work on GNNs has explored several challenges that limit their capabilities for graph learning tasks. Most prominently, the problems of over-smoothing, over-squashing, robustness and expressivity are discussed in many publications over the past eight years (Rusch et al., 2023a; Akansha, 2025; Zhang et al., 2025; Morris et al., 2019; Zhang et al., 2024; Günemann, 2022). Over-smoothing occurs when node representations become indistinguishable after many layers. Over-squashing refers to the issue where node embeddings of constant size struggle to represent information of exponentially growing receptive fields. Robustness examines a GNNs sensitivity to perturbations in input features or graph structure, with research focusing on adversarial attacks and defences. Finally, expressivity investigates the theoretical power of GNNs to distinguish between different graph structures and learn complex functions, often explored by comparing them to variants of Weisfeiler-Lehman test. While addressing all four challenges remains an active focus of current GNN research, this paper critically examines over-smoothing and over-squashing.

In a recent position paper Bechler-Speicher et al. (2025) posit that Graph Representation Learning may lose relevance due to poor benchmarks. They criticise (1) the relevance and real-world impact of learning tasks on current benchmark datasets, (2) the suitability of certain benchmark datasets for the application of GNNs, and (3) the overall benchmarking culture. Consequently, they propose a paradigm shift towards driving impactful advances in graph learning research and call for new transformative real-world applications. We anticipate that this position paper will lead

to an extensive search for such applications, potentially followed by introductions of new datasets and learning tasks, such as the very recent GraphBench (Stoll et al., 2025). Also, Coupette et al. (2025) react to Bechler-Speicher et al. (2025) by introducing a method to measure the structure and feature relevance and their relation as a notion of quality of a dataset as a graph learning benchmark. In this position paper, we advocate for additionally quantifying the relevance of theoretical phenomena as learning problems.

We believe diligent analysis of the learning tasks with statistics that measure the underlying distributions of relevant information is required to quantify theoretical problems presumed to be of practical impact and guide further directions of theoretical research. This position paper questions the practical relevance of over-smoothing and over-squashing in currently established learning tasks.

Preliminaries. Let $\mathcal{G} = (\mathcal{V}, \mathcal{E})$ be an undirected graph with node set \mathcal{V} and edge set \mathcal{E} . The graph \mathcal{G} can be represented via an adjacency matrix $\mathbf{A} \in \mathbb{R}^{|\mathcal{V}| \times |\mathcal{V}|}$ with $a_{vu} \neq 0$ if and only if $(v, u) \in \mathcal{E}$. Each node $v \in \mathcal{V}$ has a neighbourhood $\mathcal{N}(v) = \{u : (v, u) \in \mathcal{E}\}$ of degree $d(v) = |\mathcal{N}(v)|$, a k -hop neighbourhood $\mathcal{N}^{(k)}(v) = \{u \in \mathcal{V} \mid \delta(v, u) \leq k\}$, where $\delta(v, u)$ denotes the shortest path distance between v and u in the graph \mathcal{G} , and features $\mathbf{h}_v^{(0)} \in \mathbb{R}^{d_0}$, which are the rows of the matrix $\mathbf{H}^{(0)} \in \mathbb{R}^{|\mathcal{V}| \times d_0}$. Graph Neural Networks (GNNs) are neural networks designed to process graph-structured data. Most GNNs fall into the class of MPNNs, in which layers of message passing functions $M(\cdot)$ and update functions $U(\cdot)$ are iteratively composed. In layer ℓ , a new hidden embedding is computed as

$$\mathbf{h}_v^{(\ell+1)} = U \left(\mathbf{h}_v^{(\ell)}, M \left(\mathbf{h}_v^{(\ell)}, \{\mathbf{h}_u^{(\ell)} : u \in \mathcal{N}(v)\} \right) \right).$$

To exemplify this abstract function class, we consider the model equation of the GCN (Kipf & Welling, 2017) below

$$\mathbf{H}^{(\ell+1)} = \sigma \left(\tilde{\mathbf{A}} \mathbf{H}^{(\ell)} \mathbf{W}^{(\ell)} \right),$$

where the update step is defined by the non-linearity σ and learnable weight matrix $\mathbf{W}^{(\ell)}$, and the message passing step is implemented via the message passing operator $\tilde{\mathbf{A}} = (\mathbf{D} + \mathbf{I})^{-1/2} (\mathbf{A} + \mathbf{I}) (\mathbf{D} + \mathbf{I})^{-1/2}$. Note that we omit trainable bias vectors in this work for brevity. For a MPNN, the receptive field of a node v refers to the set of nodes whose initial features $\mathbf{h}^{(0)}$ influence the final embedding $\mathbf{h}_v^{(L)}$, i.e., all nodes with $\delta(v, u) \leq L$.

2. Over-Smoothing

We believe that the continued focus of theoretical research on over-smoothing within the graph learning community

constrains the practical relevance of recent contributions. In this section, we substantiate our position by first reviewing the extensive body of literature on over-smoothing, which in our view indicates that the phenomenon is both well-understood and effectively mitigated. Based on the literature, we call into question the importance of working with arbitrarily large receptive fields in current GNN research. We back our position with experiments demonstrating that even GNNs designed to avoid over-smoothing do not yield significant performance gains on standard benchmarks.

2.1. Related Work

Over-smoothing refers to the phenomenon wherein node representations converge to a single representation with an increasing number of message passing steps and hence become uninformative. In many publications, this is assumed to be the main reason for a relatively small optimal number of message passing layers compared to other neural architectures. Convolutional Neural Networks (CNNs), for example, gain performance by increasing the number of convolutions, resulting in CNN state-of-the-art architectures with hundreds of layers (He et al., 2015; Tan & Le, 2021; Howard et al., 2019).

Kipf & Welling (2017) first discovered a performance peak of GNNs, here the Graph Convolution Network (GCN), at around 7–8 message passing layers. Li et al. (2018) further investigated this phenomenon and demonstrated empirically for a small graph dataset (Zachary's karate club network (Zachary, 1977)) that repeated graph convolutions first improve the class separation in the latent space before collapsing the representations. Based on the simplification of graph convolutions as a special form of Laplacian smoothing, they show that infinitely repeated applications of the message passing operator lead node embeddings to converge to a constant vector.

Chen et al. (2019) approached the phenomenon of over-smoothing by measuring (over-)smoothness. They propose to use the Mean Average Distance (MAD) as a quantitative metric for the smoothness of the graph. The MAD applies the cosine distance to the representations of each node pair after the final layer L of the GNN. Based on this distance, they define the MADGap, the difference between remote node pairs MAD^{rmt} and neighbours MAD^{ned} , as an over-smoothness metric. Their experiments suggest a connection between over-smoothness, performance, and the information-to-noise ratio, quantified by the proportion of same-class nodes in an L -hop neighbourhood, where L corresponds to the number of message passing layers.

Oono & Suzuki (2019) investigated the asymptotic behaviour of the expressive power of GCN as the number of layers tends to infinity. They show that the node representations converge to a single signal determined by the node's

connected component and degree, as well as the exponential nature of this asymptotic behaviour, which is defined as

$$d_{\mathcal{M}}(\mathbf{h}_v^{(\ell)}) \leq s \lambda d_{\mathcal{M}}(\mathbf{h}_v^{(\ell-1)}),$$

where $d_{\mathcal{M}}(\mathbf{h}_v^{(\ell)})$ denotes the distance of the node representation \mathbf{h} in layers ℓ to the common representation in subspace \mathcal{M} of the same connected component and node degree, which measures the smoothness of the graph. The over-smoothing factor $s\lambda$ comprises λ , the non-trivial eigenvalue of the propagation matrix with the largest absolute value, and s , the largest singular value of all weight matrices $W^{(\ell)}$, or in other words, the maximum amplification factor. They argue that for most graphs, $s\lambda < 1$, implying inevitable over-smoothing.

Keriven (2022) provided a theoretical analysis of the effect of message passing, focusing not just on the asymptotic behaviour but also the optimal GNN depth. Using a stochastic latent-space random-graph model and analysing the mean-aggregation dynamics via the ergodic theorem, he showed that a limited number of message passing layers improves learning due to faster shrinking of non-principal than of principal components and compression of inter-communities variance before complete collapse occurs.

Building on the curvature-based framework for over-squashing introduced by Topping et al. (2022), Nguyen et al. (2023) connected positive edge curvature to over-smoothing. They showed that higher neighbourhood overlap between adjacent nodes implies higher curvature κ

$$\frac{|\mathcal{N}(v) \cap \mathcal{N}(u)|}{\max(d(v), d(u))} \geq \kappa(v, u),$$

and hence contributes to the smoothing of node features.

Most recently, in a preprint Keriven (2025), examined over-smoothing from an optimisation point of view. He introduces the idea of *backward over-smoothing* and argues that “as soon as the last layer of the GNN is ‘trained’, then gradients vanish at every layer and the GNN cannot train anymore”, leading to spurious stationary points.

Measuring Over-Smoothing. Several measures for over-smoothing have been proposed in recent years, which differ primarily in two design choices: (1) the metrics used to quantify the distance between node representations, and (2) the pairs of nodes between which this distance is measured. The most prominent measure is the *Dirichlet energy*, which is based on squared differences between representations of neighbouring nodes (Rusch et al., 2023a; Cai & Wang, 2020). Wu et al. (2023) propose a *node similarity* measure over all node pairs, also based on squared differences. The *Mean Average Distance* (Chen et al., 2019)

applies the cosine distance between each node and its neighbours within a given k -hop neighbourhood. We provide further details on definitions in Appendix A. To measure over-smoothing in a GNN, the appropriate distance metric must be selected depending on the message passing scheme. The degree-normalised version of the Dirichlet energy (Cai & Wang, 2020) is expected to converge to zero for GCNs, as they collapse node representations to a constant vector scaled by the degree (Oono & Suzuki, 2019; Cai & Wang, 2020). The Dirichlet energy as used by Rusch et al. (2023a) and node similarity (Wu et al., 2023) converge to zero if and only if all node representations become identical. This over-smoothing behaviour is expected for stochastic models like GATs. However, MAD can be applied to both cases, due to the application of the cosine distance.

Methodology Addressing Over-Smoothing. Several architectural interventions have been proposed to counter over-smoothing. Zhao & Akoglu (2020) introduced PairNorm to reduce the effect of over-smoothing by stabilising the sum of the distances between node pairs with and without edges. Chen et al. (2020) showed that simple skip connections can enable deep GCNs. Specifically, they introduced GCNII, which adds the initial embedding to each hidden embedding by a proportion α and an identity mapping to each weight matrix $W^{(\ell)}$ by a proportion β , where α and β are hyperparameters. Scholkemper et al. (2025) proved theoretically that a GCN incorporating both batch-normalisation and residual connections does not suffer from over-smoothing. These theoretical findings are supported by empirical results on GNN with the most common message passing methods. Rusch et al. (2023b) further developed the idea of residual layers to gradient gating (G^2) by replacing the fixed proportion β with learnable element-wise rates $\tau^{(\ell)}$. In the G^2 model, $\tau^{(\ell)}$ is given by a learnable function of the hidden features and the graph structure. Rusch et al. (2023a) surveyed these and other mitigation techniques and categorised them into: (1) normalisation and regularisation, (2) change of the GNN dynamics, and (3) architectural enhancement through residual connections. Even though they show empirically the suitability of all three approaches, the performance decreases or stagnates on the learning tasks as GNN depth increases.

The great majority of the work on over-smoothing with experimental results investigates performance degradation in association with this phenomenon only on node-level tasks, i.e., node classification.

2.2. Position

We question the negative influence of over-smoothing in real-world datasets. We consider two different cases of learning tasks with regard to the possible influence of over-smoothing, node-level tasks and graph-level tasks. For the

Table 1. Comparison of a GCN and three methods to mitigate over-smoothing for a range of model depths. The accuracy is given in %, and the computational time is given in milliseconds in brackets. The best performing model depth is highlighted in bold.

DATASET	MODEL	LAYERS					
		2	4	8	16	32	64
CORA	GCN	77.1 (3.3)	74.3 (0.4)	36.0 (12.4)	31.9 (0.0)	31.9 (0.0)	31.9 (0.0)
	GCN + PAIRNORM	69.6 (5.5)	63.9 (5.5)	60.4 (4.7)	43.0 (9.1)	36.4 (5.5)	38.5 (9.1)
	GCNII	76.3 (2.3)	75.3 (0.3)	75.7 (0.5)	75.6 (0.2)	67.3 (17.7)	76.3 (0.4)
	G^2	74.0 (2.4)	75.2 (0.4)	74.2 (0.4)	75.0 (0.4)	75.6 (1.1)	72.8 (4.0)
CITESEER	GCN	75.5 (0.8)	74.5 (0.7)	73.5 (0.4)	58.1 (12.3)	53.6 (19.2)	18.1 (0.0)
	GCN + PAIRNORM	68.2 (1.1)	68.3 (1.6)	66.4 (4.2)	63.6 (5.2)	51.6 (5.8)	21.9 (5.3)
	GCNII	76.0 (0.7)	76.4 (0.6)	76.6 (0.6)	77.4 (0.4)	77.4 (0.4)	77.6 (0.2)
	G^2	75.9 (0.5)	76.5 (0.4)	76.1 (0.4)	74.8 (3.5)	75.7 (0.5)	76.1 (0.5)
PUBMED	GCN	87.7 (0.4)	86.1 (0.2)	83.0 (4.2)	79.3 (5.6)	63.2 (11.8)	40.5 (0.4)
	GCN + PAIRNORM	87.9 (0.4)	86.4 (0.3)	85.8 (0.5)	84.7 (0.3)	84.7 (0.6)	80.2 (3.0)
	GCNII	88.3 (0.3)	88.2 (0.4)	88.4 (0.2)	88.5 (0.2)	88.2 (0.2)	88.6 (0.2)
	G^2	87.6 (1.1)	87.0 (1.5)	86.8 (2.9)	80.3 (20.9)	80.2 (20.8)	63.2 (28.6)
ROMAN-EMPIRE	GCN	41.5 (0.7)	27.3 (1.2)	18.7 (0.6)	16.5 (0.3)	15.0 (0.9)	14.6 (0.6)
	GCN + PAIRNORM	37.3 (0.4)	20.4 (0.7)	19.6 (1.1)	20.1 (1.2)	15.5 (0.8)	17.4 (3.3)
	GCNII	56.9 (1.0)	65.1 (0.6)	61.0 (0.9)	60.3 (0.2)	59.0 (0.2)	58.0 (0.5)
	G^2	62.5 (3.3)	62.9 (2.9)	60.6 (2.3)	61.2 (3.3)	61.0 (3.0)	OOM
OGBN ARXIV	GCN	55.7 (0.2)	54.2 (0.5)	32.1 (18.5)	12.2 (9.0)	7.2 (0.3)	7.0 (0.8)
	GCN + PAIRNORM	60.2 (0.3)	60.3 (0.3)	61.0 (0.2)	59.1 (0.3)	53.2 (2.8)	11.8 (4.7)
	GCNII	58.2 (0.5)	58.5 (0.6)	56.4 (2.5)	56.9 (0.3)	56.6 (0.4)	56.2 (0.2)
PHOTO	GCN	86.0 (4.5)	73.7 (8.8)	48.6 (10.0)	29.9 (12.1)	22.8 (4.4)	25.9 (2.0)
	GCN + PAIRNORM	87.0 (1.1)	78.0 (2.2)	81.7 (2.2)	81.4 (2.0)	78.7 (5.3)	65.0 (6.2)
	GCNII	86.9 (2.0)	86.5 (1.7)	85.5 (3.1)	84.5 (4.5)	85.0 (3.8)	85.1 (5.1)
	G^2	78.3 (6.2)	77.4 (10.7)	82.9 (3.3)	83.6 (3.2)	82.3 (3.3)	77.2 (4.0)
COMPUTERS	GCN	77.7 (3.7)	73.1 (4.5)	54.4 (16.3)	21.1 (14.7)	24.4 (16.8)	10.7 (12.0)
	GCN + PAIRNORM	80.7 (2.4)	75.3 (3.2)	76.0 (2.3)	65.3 (17.8)	45.5 (20.0)	59.2 (11.1)
	GCNII	81.5 (1.9)	81.3 (1.5)	81.2 (1.7)	75.1 (14.5)	80.2 (3.9)	81.2 (2.1)
	G^2	66.1 (9.9)	74.6 (4.9)	73.3 (5.9)	70.6 (9.8)	74.5 (3.7)	OOM

former, we suspect the performance decrease on real-world data often arises not from over-smoothing, but as a consequence of *uninformative receptive fields*. For most learning tasks, a small receptive field is sufficient to obtain the relevant information. If the problem radius is smaller or similar to the number of message passing steps to achieve optimal smoothing, as described by Keriven (2022), the performance will not suffer from over-smoothing. We support our position about the negligible effect of over-smoothing with experimental results in Section 2.3, which show that large model depths fail to gain significant performance improvements even if over-smoothing is prevented. For graph-level tasks, over-smoothing can even be considered beneficial if the common node representation aligns with the label distribution (Southern et al., 2025).

We furthermore want to specify that the phenomenon of over-smoothing is known to originate from the repeated application of message passing functions. Consequently, one can still fit *arbitrarily deep GNNs* without encountering over-smoothing by applying a limited number of message passing functions while working with arbitrarily deep update functions. Since, especially for large graph structures, the

implementation of message passing comes at a significant computational expense, we posit that the desire to perform arbitrarily many message passing operations is not aligned with the practical deployment of GNNs.

Finally, we want to highlight that scaling the performance of GNNs to a very large number of message passing operations may be misguided due to the *methodological alternatives* that have been developed over the past years. Specifically, for problems with a very large problem radius, i.e., problems that justify the consideration of a very large receptive field per node, one may almost surely want to explore alternatives such as Graph Transformers (Kreuzer et al., 2021; Ying et al., 2021; Rampášek et al., 2022) or rewiring techniques (Deac et al., 2022; Karhadkar et al., 2023; Arnaiz-Rodríguez et al., 2022) to consider these large receptive fields more efficiently than to perform as many or more message passing operations than the problem radius.

Outlook. As a consequence of the questionable practical relevance of over-smoothing, the graph learning community should focus its efforts on phenomena of proven relevance implied by the conditions in given learning tasks and

datasets. We suggest it might be helpful to develop statistics that quantify the label relevance of different-sized receptive fields. This quantification of the problem radius, in combination with an observation of the optimal smoothing depth, should guide our efforts in improving model architectures.

Other Positions. In parallel and independent work [Arnaiz-Rodriguez & Errica \(2025\)](#) challenge common beliefs by constructing theoretically sound counterexamples. In one of their positions, they question the performance-degrading effect of over-smoothing, which aligns with our arguments and experimental results. While we suspect uninformative receptive fields as a reason for limited performance in deep GNNs and call for measuring the relevance of label distributions, they emphasise the importance of node separability, which can be influenced by many effects and suggest further research efforts in this direction. Furthermore, [Park et al. \(2025\)](#) posit that “over-smoothing has been confused with the vanishing gradient” and call for research on the question of whether shallow optimal depth is inherent to GNNs, whereas we advocate for a more problem-oriented approach to allocate research efforts guided by statistics that measure if theoretical phenomena like over-smoothing result in practical problems.

2.3. Empirical Findings

We support our position on over-smoothing with experimental results, which show that mitigation techniques in most cases prevent models from over-smoothing, but do not score significantly better results with increasing model depth.

We conducted experiments using a standard GCN and three models designed to mitigate over-smoothing, namely a GCN with PairNorm ([Zhao & Akoglu, 2020](#)), a GCNII ([Chen et al., 2020](#)), and a G²-GCN ([Rusch et al., 2023b](#)), on common node-classification datasets. For each model–dataset combination, we performed hyperparameter optimisation and training, and then evaluated both the classification performance and relevant over-smoothing measures for an exponentially increasing number of message passing layers, ranging from 2 to 64. Appendix B provides more details about the experimental set-up.

The results clearly show that over-smoothing is of negligible relevance in the examined datasets. Although the mitigation techniques successfully prevent over-smoothing, they do not improve performance. For the GCN with an increasing number of message passing layers, we can observe a performance decrease in Table 1 as well as a decreasing MAD in Figure 1. A concurrency of these effects, like on Cora in the 8th layer or for PubMed in the 32nd and 64th layer, could indicate over-smoothing. However, on other datasets, like Roman-Empire and Photo, the drop in performance precedes that in MAD, which could be explained

by an uninformative receptive field. In contrast, the GCNII and the G²-GCN, which are theoretically capable of compensating for over-smoothing and uninformative receptive fields, exhibit none of these behaviours, maintaining relatively stable accuracy and MAD across layers. PairNorm at least reduces the effect, resulting in a more moderate decline. However, in most cases, the optimal performance is achieved with a shallow model. In those cases where the best accuracy is obtained with a large number of layers, the improvement is marginal and does not justify the increasing computational cost. These findings are consistent across additional experiments using GATv2 and GraphSAGE as message passing mechanisms, as detailed in Appendix C. These results provide empirical support for our position, stating that the practical effects of over-smoothing are negligible.

A Remark on the Over-Smoothing Measures. In Figure 1, we observe that the Dirichlet energy for the GCN does not exhibit the expected exponential decrease reported for node-similarity-based measures in other works ([Rusch et al., 2023a; Park et al., 2025; Wu et al., 2023](#)), whereas MAD does to some extent. This suggests that the angle between the representations decreases while their magnitudes increase. These different experimental results may arise from conducting hyperparameter tuning and model training for the experimental study in this work. These findings are consistent with empirical works that show that a simple scaling of the weight matrices ([Arnaiz-Rodriguez & Errica, 2025; Roth & Liebig, 2024](#)) prevents a collapse of the Dirichlet energy.

3. Over-Squashing

We believe that continued theoretical work on over-squashing should be guided by measurable problems that limit the performance of GNNs in practical applications. In this section, we base our position on the literature, reviewing different perspectives on the phenomenon. We address these perspectives and, as a consequence, question the relevance of over-squashing for practical applications. We support our position with experimental results showing no consistent improvement of the accuracy after mitigating over-squashing.

3.1. Related Work

Over-squashing refers to the extensively studied phenomenon in which too much information is forced to pass through overly small node embeddings. If a node v is to be affected by features of node u at distance k , a GNN requires at least k message passing steps. However, an increasing number of message passings results in an exponentially growing number of messages being sent, leading

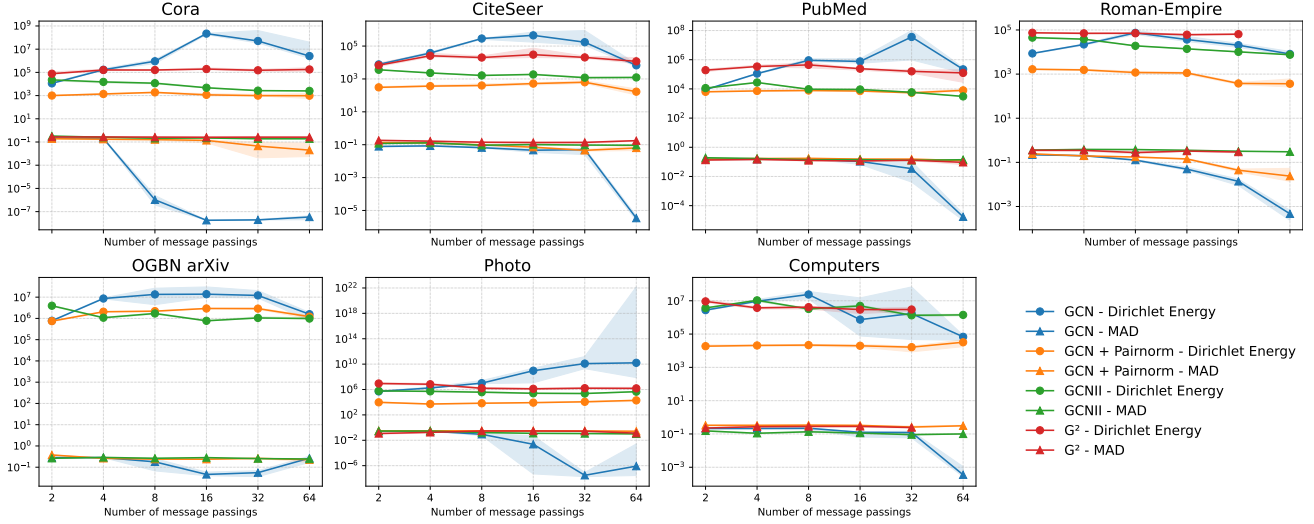


Figure 1. MAD with a 3-hop neighbourhood and Dirichlet energy of the whole dataset for all tested models and datasets at different depths after hyperparameter tuning and training. The error bands represent the 25- and 75-percentiles.

to a loss of information. In other words, over-squashing can be defined as the inability to losslessly compress a receptive field that grows with the depth of the network in fixed-sized node representations. As a consequence of over-squashing, features from neighbours in different k -hops can not be considered jointly at the central node, preventing the modelling of interaction effects. In detail, the phenomenon of over-squashing has been defined in various ways, focusing on different aspects of the phenomenon.

The concept of over-squashing was introduced by [Alon & Yahav \(2020\)](#) with the broadest definition of over-squashing. Based on the exponential growth of the receptive field of a node v with the number of message passing $|\mathcal{N}^{(L)}(v)| = \mathcal{O}(e^L)$, they conclude an over-squashing of an exponentially growing amount of information while the embedding dimension remains constant. They emphasise the increasing severity of this phenomenon for problems that require *long-range information*, i.e., with a large problem radius r . With a synthetic dataset, [Alon & Yahav \(2020\)](#) showed the limitation of GNNs with the most common message passing methods for large problem radii and attributed this to over-squashing. Additionally, they validated their results on a real-world dataset and showed that for a GNN with $L = 8$ and using fully-adjacent layers, which theoretically prevents over-squashing, improved the results practically.

[Topping et al. \(2022\)](#) investigate over-squashing through *graph curvature*, focusing on bottleneck edges that induce over-squashing locally. They formulate the over-squashing phenomenon as an upper bound for the entries in the *Jacobian* and define it for the derivative of the hidden feature $h_v^{(r+1)}$ with respect to an input feature $h_u^{(0)}$ between a node

v and another node u with $\delta(v, u) = r$ as

$$\left| \frac{\partial h_v^{(r+1)}}{\partial h_u^{(0)}} \right| \leq (\alpha \cdot \beta)^{r+1} (\tilde{A}^{r+1})_{v,u}, \quad (1)$$

with the layer-wise Lipschitz constants $|\Delta U^{(\ell)}| \leq \alpha$ and $|\Delta M^{(\ell)}| \leq \beta$ for $0 \leq \ell \leq r$. The factor $(\tilde{A}^{r+1})_{v,u}$ causes vanishing gradients, especially with bottleneck edges on the path between the two nodes. [Topping et al. \(2022\)](#) propose a modified Forman curvature, which uses the counts of triangles and 4-cycles based on an edge, to identify bottlenecks.

[Di Giovanni et al. \(2023\)](#) extended the fundamental understanding of over-squashing by investigating its impact on the width, depth and topology, viewing small magnitudes of Jacobian entries between features of a node v and another node u with a long-range interaction in general as a problem of over-squashing. They defined an alternative upper bound for the L_1 -Norm of the Jacobian, which differs slightly from Equation (1) and is defined as

$$\left\| \frac{\partial \mathbf{h}_v^{(\ell)}}{\partial \mathbf{h}_u^{(0)}} \right\|_{L_1} \leq \underbrace{(c_\sigma \cdot w \cdot p)}_{\text{model}}^\ell \underbrace{(\tilde{A}^\ell)_{v,u}}_{\text{topology}}, \quad (2)$$

where c_σ is the Lipschitz constant of the nonlinearity σ , w is the maximal entry-value over all weight matrices, and p is the hidden dimension or model width. They derive from Equation (2) that a larger hidden dimension prevents over-squashing if it compensates for the topology factor. However, they point out that an increased hidden dimension

reduces the ability of generalisation and does not solve the actual problem, the graph topology. Further, they prove for tasks with long-range dependencies, i.e., large problem radii r , the occurrence of over-squashing for models with a depth comparable to the problem radius ($L \approx r$) and vanishing gradients for deeper models ($L \gg r$). Lastly, Di Giovanni et al. (2023) add another perspective on over-squashing and show that it occurs for a pair of nodes $v, u \in \mathcal{V}$ with a high commute time π , which measures the expected number of steps for a random walk to commute between v and u .

Methodology Addressing Over-Squashing. Topping et al. (2022) introduce a curvature-based rewiring method incorporating their Balanced Forman metric to reduce over-squashing on bottlenecks. The *Stochastic Discrete Ricci Flow* (SDRF) adds edges to support low-curvature edges and removes high-curvature edges. A similar approach called *Batch Ollivier-Ricci Flow* (BORF) was proposed by Nguyen et al. (2023), using the Ollivier-Ricci curvature

$$\kappa(v, u) = \frac{W_1(\mu_v, \mu_u)}{\delta(v, u)},$$

where $W_1(\mu_v, \mu_u)$ is the L1-Wasserstein distance and $\delta(v, u)$ is the shortest path distance. They use κ for adding and removing edges in the graph to simultaneously mitigate over-squashing and over-smoothing, respectively. Deac et al. (2022) create a modified graph structure using a fundamentally sparse family of expander graphs with a low diameter. In the Graph Expander Propagation (EGP), they replace \mathcal{E} for every second propagation step with edges from the expander, reducing effective path lengths. Southern et al. (2025) build upon the observations of Di Giovanni et al. (2023) that over-squashing comes with long-range dependencies with long commute times and show theoretically and empirically that a virtual node can reduce π and therefore reduce over-squashing.

3.2. Position

We challenge the presumed detrimental effect of over-squashing in real-world applications. More specifically, we question the practical relevance of joint observations of entire receptive fields, long-range interactions, and information exchange through bottlenecks. We now discuss our position on these three concrete over-squashing definitions in turn.

The formulation of the over-squashing phenomenon through a limit of the Jacobian is based on the assumption that *long-range interactions* are generally informative for learning tasks and desirable to achieve through deep GNNs. We posit that in most practical applications on a reasonably constructed graph, the relevant information on interaction effects is stored within a small k -hop neighbourhood.

Next, we challenge the negative effect of low-curvature edges. *Bottleneck edges* limit the exchange of information between structural communities. An interrelation between negative curvature between these communities and the label distribution has not been investigated yet. However, we assume in most cases a correlation between these. Information exchange along bottleneck edges is not relevant for such learning tasks.

At last, we consider the most general formulation of the over-squashing phenomenon, that is, the exponentially growing receptive field and the presumed impossibility of summarising its information in a constant hidden dimension. Implicit in this definition of over-squashing is the assumption that the information of the *entire receptive field* needs to be jointly observed to perform the given learning task. In other words, the impossibility definition states that the joint distribution over the receptive field of a node does not factorise into marginal distributions over the nodes, i.e., we assume the presence of high-order interaction effects within the receptive field of a node. We posit that this assumption is unrealistic and that for most real-world datasets, the joint distribution over the receptive field of a node does factorise and that we can hence process subsets of the receptive field independently and efficiently. In essence, it seems to us that a fixed-size node representation should be sufficient to successfully complete the majority of learning tasks for arbitrarily large receptive fields on real-world datasets.

We support our assumptions with experimental results presented in Section 3.3. The findings suggest that negative curvature does not limit predictive performance.

Outlook. We suggest a diligent analysis of future learning tasks and datasets for a better understanding of the feature, structure and label distributions and their interplay. Statistics are required to measure the localisation and factorisation of the label distribution conditioned on the structure and feature information. In addition to the relevant problem radius as proposed in Section 2.2, we suggest investigating the *specific localisation* of relevant information, which can help understand interaction along low-curvature edges and long-range relationships, to guide targeted rewiring techniques. First attempts have been made to measure this through the calculation of the Jacobian (Bamberger et al., 2025; Liang et al., 2025). However, this statistic lacks diagnostic precision due to the overlapping effects of the model definition and underlying structure. To us, it seems preferable to separately establish the presence of potential over-squashing effects in the underlying graph structure and in the different models that could be applied to this graph data. We furthermore want to specify that the definition of over-squashing via the Jacobian and the related remedy of rewiring operate under the assumption that single nodes, often at a large shortest path distance, contain information that is uniquely

Table 2. Comparison in node-classification of a GCN and three methods to mitigate over-squashing for a range of model depths. The accuracy is given in %, and the computational time is given in milliseconds in brackets. Missing combinations of dataset and model are OOM for 251 GB RAM. The best performing model is highlighted in bold. The optimal depth per model and dataset is underlined.

DATASET	MODEL	LAYERS					
		2	4	8	16	32	64
CORA	GCN	<u>77.1 (3.3)</u>	74.3 (0.4)	36.0 (12.4)	31.9 (0.0)	31.9 (0.0)	31.9 (0.0)
	EGP (GCN)	77.7 (4.7)	31.9 (0.0)	31.9 (0.0)	31.9 (0.0)	31.9 (0.0)	31.9 (0.0)
	GCN + BORF	<u>75.4 (0.3)</u>	71.3 (6.9)	35.9 (11.9)	31.9 (0.0)	31.9 (0.0)	31.9 (0.0)
	GCN + SDRF	<u>76.2 (3.0)</u>	36.1 (12.6)	34.2 (7.0)	31.9 (0.0)	31.9 (0.0)	31.9 (0.0)
CITESEER	GCN	<u>75.5 (0.8)</u>	74.5 (0.7)	73.5 (0.4)	58.1 (12.3)	53.6 (19.2)	18.1 (0.0)
	EGP (GCN)	<u>75.7 (0.6)</u>	63.8 (4.8)	42.6 (2.0)	20.5 (4.4)	18.5 (1.5)	18.7 (2.0)
	GCN + BORF	<u>75.9 (0.5)</u>	74.5 (0.7)	73.4 (0.7)	69.7 (4.7)	57.5 (14.0)	24.3 (9.2)
	GCN + SDRF	76.1 (0.6)	74.8 (0.7)	73.4 (0.6)	66.4 (5.5)	52.0 (18.9)	OOM
PUBMED	GCN	87.7 (0.4)	86.1 (0.2)	83.0 (4.2)	79.3 (5.6)	63.2 (11.8)	40.5 (0.4)
	EGP (GCN)	<u>87.1 (0.4)</u>	86.8 (0.4)	69.1 (9.5)	40.5 (0.4)	40.4 (0.2)	40.4 (0.3)
	GCN + BORF	<u>87.7 (0.4)</u>	85.9 (0.4)	84.0 (3.2)	75.9 (12.7)	68.6 (7.8)	40.4 (0.6)
	GCN + SDRF	<u>87.7 (0.3)</u>	86.0 (0.4)	85.0 (0.3)	77.9 (5.1)	47.0 (12.5)	40.6 (0.2)
ROMAN-EMPIRE	GCN	41.5 (0.7)	27.3 (1.2)	18.7 (0.6)	16.5 (0.3)	15.0 (0.9)	14.6 (0.6)
	EGP (GCN)	41.9 (0.2)	21.9 (0.6)	14.1 (0.2)	14.3 (0.4)	14.6 (0.9)	14.7 (1.1)
	GCN + BORF	<u>40.9 (0.7)</u>	26.7 (0.7)	18.8 (0.7)	16.5 (0.3)	15.1 (0.5)	14.4 (0.6)
	GCN + SDRF	<u>41.6 (0.7)</u>	27.3 (1.1)	18.5 (0.5)	16.4 (0.3)	15.1 (0.7)	14.7 (1.2)
OGBN ARXIV	GCN	<u>55.7 (0.2)</u>	54.2 (0.5)	32.1 (18.5)	12.2 (9.0)	7.2 (0.3)	7.0 (0.8)
	EGP (GCN)	57.6 (0.3)	23.8 (10.3)	6.7 (0.4)	7.8 (0.3)	7.2 (0.7)	6.9 (1.2)
PHOTO	GCN	86.0 (4.5)	73.7 (8.8)	48.6 (10.0)	29.9 (12.1)	22.8 (4.4)	25.9 (2.0)
	EGP (GCN)	<u>77.9 (13.1)</u>	56.2 (15.9)	32.1 (9.2)	24.3 (1.8)	25.1 (1.7)	27.1 (3.0)
	GCN + BORF	<u>82.0 (5.7)</u>	71.9 (14.9)	53.1 (15.4)	31.1 (8.1)	28.9 (12.0)	25.9 (1.3)
	GCN + SDRF	<u>85.8 (4.1)</u>	79.1 (6.4)	53.3 (16.3)	35.1 (13.4)	29.0 (8.8)	26.0 (1.3)
COMPUTERS	GCN	<u>77.7 (3.7)</u>	73.1 (4.5)	54.4 (16.3)	21.1 (14.7)	24.4 (16.8)	10.7 (12.0)
	EGP (GCN)	81.3 (1.6)	73.5 (1.8)	11.6 (9.8)	3.3 (2.4)	3.9 (2.2)	3.9 (3.2)
	GCN + SDRF	<u>76.1 (2.6)</u>	72.4 (4.2)	64.5 (4.6)	25.4 (17.9)	26.1 (18.6)	9.6 (11.0)

relevant to accurately represent a considered central node. It seems to us that further research on this phenomenon should formally define structures in which such far-removed nodes do contain information that is relevant to the representation of different nodes in the graph, and that real-world examples, in which such phenomena can be observed and measured, should be found. The extension of the work by Bamberger et al. (2025) and Liang et al. (2025) to not only record the average Jacobian over k -hop neighbourhoods, but to also look for outliers in the Jacobian values in the k -hop neighbourhoods could be a starting point for such research, since it may permit the identification of individual nodes at a potentially large distance, which may go unnoticed if one averages over entire k -hops (even if as specified earlier, it may be preferable to measure such effects for the model and underlying graph structure separately).

Moreover, we suggest exploring potential *factorisation* of the label distribution over k -hop receptive fields to assess the importance of a joint observation of the whole receptive field. The quantification of interaction effects in receptive fields of nodes has the potential to not only guide the development of future GNNs that are more closely aligned with the challenges posed by impactful, real-world learning prob-

lems, but also to offer an insightful categorisation of existing datasets and the ability of models to capture such effects. The application of these statistics shall allow us to better understand the practical implications of these phenomena and to set the right focus for further research directions.

Other Positions. Arnaiz-Rodriguez & Errica (2025) criticise the current definition of over-squashing as inconsistent, which is compatible with our view. They decompose the over-squashing phenomenon into topological and computational bottlenecks, whereas we use a slightly different decomposition to structure our arguments. Our position on low-curvature edges aligns with their view on the relevance of topological bottlenecks in long-range tasks. While they call for synthetic datasets, like in Mathys et al. (2025), to investigate both types of bottlenecks separately, we call for research on measuring the different aspects of over-squashing in real-world datasets. Both share the same goal of better understanding these phenomena and their impact on GNNs.

Table 3. Comparison in graph-classification of a GIN and two methods to mitigate over-squashing for a range of model depths. The accuracy (or average precision for Peptides-func) is given in %, and the computational time is given in milliseconds in brackets. The best performing model is highlighted in bold. The optimal depth per model and dataset is underlined.

DATASET	MODEL	LAYERS					
		2	4	8	16	32	64
MUTAG	GIN	87.7 (3.1)	86.3 (3.3)	84.2 (2.2)	86.7 (3.0)	84.4 (3.9)	88.2 (3.7)
	EGP (GIN)	91.1 (1.4)	74.6 (11.2)	61.1 (8.0)	65.8 (2.3)	63.9 (6.1)	<u>66.0 (3.5)</u>
	GIN + BORF	88.1 (2.7)	86.5 (2.0)	86.1 (1.7)	87.0 (3.9)	83.2 (4.9)	83.5 (5.2)
	GIN + SDRF	89.5 (2.6)	86.3 (3.0)	81.9 (3.0)	82.3 (7.3)	88.1 (3.9)	86.5 (3.8)
ENZYMES	GIN	60.6 (3.4)	59.0 (1.4)	56.8 (3.2)	47.7 (4.3)	31.0 (3.6)	17.7 (2.5)
	EGP (GIN)	<u>50.2 (2.7)</u>	45.3 (3.8)	24.7 (3.5)	18.8 (4.4)	17.9 (3.3)	16.6 (0.4)
	GIN + BORF	<u>56.9 (2.4)</u>	<u>58.4 (2.1)</u>	57.6 (2.0)	47.1 (3.0)	30.5 (3.7)	19.1 (2.9)
	GIN + SDRF	50.3 (2.6)	<u>48.4 (2.3)</u>	44.6 (2.7)	35.9 (3.0)	27.0 (3.1)	16.4 (1.8)
PROTEINS	GIN	64.0 (1.1)	64.3 (1.3)	64.2 (1.3)	63.9 (1.2)	<u>66.5 (2.2)</u>	66.1 (1.9)
	EGP (GIN)	61.8 (0.7)	<u>65.6 (2.2)</u>	65.7 (3.4)	<u>68.1 (8.6)</u>	<u>41.0 (15.5)</u>	46.8 (18.2)
	GIN + BORF	65.3 (1.2)	63.7 (1.0)	<u>72.6 (1.9)</u>	65.6 (2.1)	66.9 (2.1)	68.0 (1.4)
	GIN + SDRF	70.3 (0.9)	72.0 (1.3)	<u>72.9 (1.8)</u>	72.8 (2.0)	71.4 (2.0)	68.1 (1.9)
PEPTIDES-FUNC	GIN	59.3 (0.5)	60.7 (1.0)	57.9 (1.1)	60.7 (1.1)	55.7 (1.2)	42.2 (8.5)
	EGP (GIN)	41.6 (0.3)	<u>42.9 (0.6)</u>	21.4 (3.2)	17.5 (0.2)	17.3 (0.3)	17.2 (0.4)
	GIN + BORF	59.0 (0.8)	<u>59.7 (0.6)</u>	57.9 (1.4)	55.8 (1.4)	49.7 (0.8)	47.0 (1.4)
	GIN + SDRF	56.7 (0.6)	<u>55.2 (0.8)</u>	53.1 (0.7)	53.8 (1.0)	49.8 (1.5)	40.4 (4.1)

Table 4. Regression results of one curvature value on the predictive performance for each dataset. Statistical significance is indicated using stars, with * denoting $p < 0.05$ and ** denoting $p < 0.005$.

Dataset	Balanced Forman Curvature		Ollivier-Ricci Curvature	
	Slope	p-Value	Slope	p-Values
Cora	0.011	0.441	0.026	0.455
CiteSeer	0.004	0.248	0.018	0.256
PubMed	-0.002	0.553	-0.003	0.552
Roman-Empire	0.015	0.743	0.046	0.734
Photo	-0.039	0.005**	-0.086	0.005**
Computers	-0.005	0.685	-0.011	0.686
Mutag	0.047	0.001**	-0.06	0.324
Enzymes	0.344	0.009*	-0.143	0.09
Proteins	-0.05	0.02*	0.063	0.119
Peptides-func	0.028	0.562	0.255	0.027*

3.3. Empirical Findings

In this section, we demonstrate that, in practical applications, there is no significant relationship between the reduction of measurable over-squashing and predictive performance.

We investigate the potential of over-squashing mitigation techniques, namely EGP (Deac et al., 2022), BORF (Nguyen et al., 2023), and SDRF (Topping et al., 2022), in combination with various message passing methods on common node-level and graph-level tasks, by performing hyperparameter optimisation and training as described in Section 2.3. Furthermore, we evaluate the Balanced Forman and Ollivier-Ricci curvature discussed in Section 3.1 on the original graphs and the graphs modified by the mitigation techniques. This currently constitutes the only available method to quan-

tify over-squashing. To assess the impact of curvature reduction on predictive performance, we fit a linear regression for each dataset, using accuracy as the dependent variable and the curvature as the independent variable. Appendix D contains further information on the curvature evaluation.

Considering the results in Tables 2 and 3, we observe that neither the individual approaches nor graph rewiring in general consistently improves model accuracy. Further results for all message passing methods are provided in Appendix C. Moreover, as shown in Table 4, for none of the tested datasets are both estimated slope coefficients of curvature on predictive performance significantly greater than zero. We can conclude from these results that local over-squashing through structural bottlenecks does not significantly limit predictive performance on common benchmark datasets.

4. Conclusion

In this position paper, we highlight the importance of an in-depth understanding of real-world learning problems to guide future research directions in theoretical work in graph representation learning. While much excellent work has been done to better understand and solve over-squashing and over-smoothing, the practical relevance of these phenomena should be questioned. As Bechler-Speicher et al. (2025) recently criticised the current benchmarking culture and called for new transformative real-world benchmarking datasets, we hope that many new learning tasks with individual challenges will emerge and gain importance. It seems crucial to us that, as part of this search for new appli-

cations and datasets, we analyse these diligently, especially for topics like over-smoothing and over-squashing. Statistics should be established to measure the localisation and factorisation of the feature, structure and label distributions.

Acknowledgements

We thank sincerely Federico Errica and Adrian Arnaiz-Rodriguez for insightful discussions about our understanding over-smoothing and over-squashing. The work of Niklas Kormann, Benjamin Doerr and Johannes Lutzeyer was supported by the ANR PRC HistoGraph grant (ANR-23-CE45-0038). This work was granted access to the HPC resources of IDRIS under the allocation “AD011016620” made by GENCI.

References

Akansha, S. Over-squashing in graph neural networks: A comprehensive survey. *Neurocomputing*, 642:130389, 2025.

Alon, U. and Yahav, E. On the bottleneck of graph neural networks and its practical implications. In *International Conference on Learning Representations (ICRL)*, 2020.

Arnaiz-Rodriguez, A. and Errica, F. Oversmoothing, over-squashing, heterophily, long-range, and more: Demystifying common beliefs in graph machine learning. In *arXiv*, 2025.

Arnaiz-Rodríguez, A., Begga, A., Escolano, F., and Oliver, N. Diffwire: Inductive graph rewiring via the lovász bound. In *Learning on Graphs Conference (LOG)*, 2022.

Bamberger, J., Gutteridge, B., le Roux, S., Bronstein, M. M., and Dong, X. On measuring long-range interactions in graph neural networks. In *International Conference on Machine Learning (ICML)*, 2025.

Bechler-Speicher, M., Finkelshtein, B., Frasca, F., Müller, L., Tönshoff, J., Siraudin, A., Zaverkin, V., Bronstein, M., Niepert, M., Perozzi, B., Galkin, M., and Morris, C. Position: Graph learning will lose relevance due to poor benchmarks. In *International Conference on Machine Learning (ICML)*, 2025.

Brody, S., Alon, U., and Yahav, E. How attentive are graph attention networks? In *International Conference on Learning Representations (ICRL)*, 2022.

Cai, C. and Wang, Y. A note on over-smoothing for graph neural networks. In *Graph Representation Learning and Beyond Workshop, ICML*, 2020.

Chen, D., Lin, Y., Li, W., Li, P., Zhou, J., and Sun, X. Measuring and relieving the over-smoothing problem for graph neural networks from the topological view. In *AAAI Conference on Artificial Intelligence*, 2019.

Chen, M., Wei, Z., Huang, Z., Ding, B., and Li, Y. Simple and deep graph convolutional networks. In *International Conference on Machine Learning (ICML)*, 2020.

Coupette, C., Wayland, J., Simons, E., and Rieck, B. No metric to rule them all: Toward principled evaluations of graph-learning datasets. In *International Conference on Machine Learning (ICML)*, 2025.

Deac, A., Lackenby, M., and Veličković, P. Expander graph propagation. In *Advances in Neural Information Processing Systems (NeurIPS)*, 2022.

Derrow-Pinion, A., She, J., Wong, D., Lange, O., Hester, T., Perez, L., Nunkesser, M., Lee, S., Guo, X., Wiltshire, B., Battaglia, P. W., Gupta, V., Li, A., Xu, Z., Sanchez-Gonzalez, A., Li, Y., and Velickovic, P. ETA prediction with graph neural networks in google maps. In *ACM International Conference on Information & Knowledge Management*, 2021.

Di Giovanni, F., Giusti, L., Barbero, F., Luise, G., Lio', P., and Bronstein, M. On over-squashing in message passing neural networks: The impact of width, depth, and topology. In *Transactions on Machine Learning Research*, 2023.

Dwivedi, V. P., Rampášek, L., Galkin, M., Parviz, A., Wolf, G., Luu, A. T., and Beaini, D. Long range graph benchmark. In *Advances in Neural Information Processing Systems (NeurIPS)*, 2023.

Errica, F., Podda, M., Bacciu, D., and Micheli, A. A fair comparison of graph neural networks for graph classification. In *International Conference on Learning Representations (ICRL)*, 2020.

Gilmer, J., Schoenholz, S. S., Riley, P. F., Vinyals, O., and Dahl, G. E. Neural message passing for quantum chemistry. In *International Conference on Machine Learning (ICML)*, 2017.

Günnemann, S. *Graph Neural Networks: Adversarial Robustness*, pp. 149–176. 2022. ISBN 978-981-16-6053-5.

He, K., Zhang, X., Ren, S., and Sun, J. Deep residual learning for image recognition. In *IEEE Conference on Computer Vision and Pattern Recognition*, 2015.

Howard, A., Pang, R., Adam, H., Le, Q. V., Sandler, M., Chen, B., Wang, W., Chen, L., Tan, M., Chu, G., Vasudevan, V., and Zhu, Y. Searching for MobileNetV3. In *International Conference on Computer Vision (ICCV)*, 2019.

Hu, W., Fey, M., Zitnik, M., Dong, Y., Ren, H., Liu, B., Catasta, M., and Leskovec, J. Open graph benchmark: Datasets for machine learning on graphs. *Advances in Neural Information Processing Systems (NeurIPS)*, 2020.

Ivanov, S., Sviridov, S., and Burnaev, E. Understanding isomorphism bias in graph data sets. In *arXiv*, 2019.

Karhadkar, K., Banerjee, P. K., and Montúfar, G. Fosr: First-order spectral rewiring for addressing oversquashing in gnns. In *International Conference on Learning Representations (ICLR)*, 2023.

Keriven, N. Not too little, not too much: a theoretical analysis of graph (over)smoothing. In *Advances in Neural Information Processing Systems (NeurIPS)*, 2022.

Keriven, N. Backward oversmoothing: Why is it hard to train deep graph neural networks? In *arXiv*, 2025.

Kipf, T. N. and Welling, M. Semi-supervised classification with graph convolutional networks. In *International Conference on Learning Representations (ICRL)*, 2017.

Kreuzer, D., Beaini, D., Hamilton, W., Létourneau, V., and Tossou, P. Rethinking graph transformers with spectral attention. *Advances in Neural Information Processing Systems (NeurIPS)*, 34:21618–21629, 2021.

Li, Q., Han, Z., and Wu, X.-M. Deeper insights into graph convolutional networks for semi-supervised learning. In *AAAI on Artificial Intelligence*, 2018.

Li, S., Zhou, J., Xu, T., Dou, D., and Xiong, H. Geomgcl: Geometric graph contrastive learning for molecular property prediction. *AAAI Conference on Artificial Intelligence*, 2021.

Liang, H., de Ocáriz Borde, H. S., Sripathmanathan, B., Bronstein, M., and Dong, X. Towards quantifying long-range interactions in graph machine learning: A large graph dataset and a measurement. In *arXiv*, 2025.

Liu, P., Wei, H., Hou, X., Shen, J., He, S., Shen, K. Q., Chen, Z., Borisyuk, F., Hewlett, D., Wu, L., Veeraraghavan, S., Tsun, A., Jiang, C., and Zhang, W. LinkSAGE: Optimizing job matching using graph neural networks. In *ACM International Conference on Knowledge Discovery & Data Mining*, 2024.

Mathys, J., Christiansen, H., Errica, F., and Alesiani, F. Long-range ising model: A benchmark for long-range capabilities in graph learning, 2025.

Morris, C., Ritzert, M., Fey, M., Hamilton, W. L., Lenssen, J. E., Rattan, G., and Grohe, M. Weisfeiler and leman go neural: Higher-order graph neural networks. In *AAAI Conference on Artificial Intelligence*, 2019.

Morris, C., Kriege, N. M., Bause, F., Kersting, K., Mutzel, P., and Neumann, M. Tudataset: A collection of benchmark datasets for learning with graphs. In *Graph Representation Learning and Beyond Workshop, ICML*, 2020.

Nguyen, K., Nong, H., Nguyen, V., Ho, N., Osher, S., and Nguyen, T. Revisiting over-smoothing and over-squashing using ollivier-ricci curvature. In *International Conference on Machine Learning (ICML)*, 2023.

Oono, K. and Suzuki, T. Graph neural networks exponentially lose expressive power for node classification. In *International Conference on Learning Representations (ICRL)*, 2019.

Park, M., Choi, S., Heo, J., Park, E., and Kim, D. The oversmoothing fallacy: A misguided narrative in gnn research, 2025.

Platonov, O., Kuznedelev, D., Diskin, M., Babenko, A., and Prokhortenkova, L. A critical look at the evaluation of gnns under heterophily: Are we really making progress? In *International Conference on Learning Representations (ICRL)*, 2024.

Rampášek, L., Galkin, M., Dwivedi, V. P., Luu, A. T., Wolf, G., and Beaini, D. Recipe for a general, powerful, scalable graph transformer. *Advances in Neural Information Processing Systems (NeurIPS)*, 2022.

Roth, A. and Liebig, T. Rank collapse causes over-smoothing and over-correlation in graph neural networks. In *Learning on Graphs Conference*, 2024.

Rusch, T. K., Bronstein, M. M., and Mishra, S. A survey on oversmoothing in graph neural networks. In *arXiv*, 2023a.

Rusch, T. K., Chamberlain, B. P., Mahoney, M. W., Bronstein, M. M., and Mishra, S. Gradient gating for deep multi-rate learning on graphs. In *International Conference on Learning Representations (ICRL)*, 2023b.

Scholkemper, M., Wu, X., Jadbabaie, A., and Schaub, M. T. Residual connections and normalization can provably prevent oversmoothing in gnns. In *International Conference on Learning Representations (ICRL)*, 2025.

Shchur, O., Mumme, M., Bojchevski, A., and Günnemann, S. Pitfalls of graph neural network evaluation. In *Relational Representation Learning Workshop, NeurIPS*, 2018.

Southern, J., Giovanni, F. D., Bronstein, M., and Lutzeyer, J. F. Understanding virtual nodes: Oversquashing and node heterogeneity. In *International Conference on Learning Representations (ICRL)*, 2025.

Stoll, T., Qian, C., Finkelshtein, B., Parviz, A., Weber, D., Frasca, F., Shavit, H., Sirauidin, A., Mielke, A., Anasta-cio, M., Müller, E., Bechler-Speicher, M., Bronstein, M., Galkin, M., Hoos, H., Niepert, M., Perozzi, B., Tönshoff, J., and Morris, C. Graphbench: Next-generation graph learning benchmarking. In *arXiv*, 2025.

Tan, M. and Le, Q. V. EfficientNetV2: Smaller models and faster training. In *International Conference on Machine Learning (ICML)*, 2021.

Topping, J., Giovanni, F. D., Chamberlain, B. P., Dong, X., and Bronstein, M. M. Understanding over-squashing and bottlenecks on graphs via curvature. In *International Conference on Learning Representations (ICRL)*, 2022.

Veličković, P., Cucurull, G., Casanova, A., Romero, A., Liò, P., and Bengio, Y. Graph attention networks. In *International Conference on Learning Representations (ICRL)*, 2018.

Wu, X., Ajourlou, A., Wu, Z., and Jadbabaie, A. Demystifying oversmoothing in attention-based graph neural networks. In *Advances in Neural Information Processing Systems (NeurIPS)*, 2023.

Yang, Z., Cohen, W. W., and Salakhutdinov, R. Revisiting semi-supervised learning with graph embeddings. In *International Conference on Machine Learning (ICML)*, 2016.

Ying, C., Cai, T., Luo, S., Zheng, S., Ke, G., He, D., Shen, Y., and Liu, T.-Y. Do transformers really perform badly for graph representation? *Advances in Neural Information Processing Systems (NeurIPS)*, 34:28877 – 28888, 2021.

Ying, R., He, R., Chen, K., Eksombatchai, P., Hamilton, W. L., and Leskovec, J. Graph convolutional neural networks for web-scale recommender systems. In *ACM International Conference on Knowledge Discovery & Data Mining*. ACM, 2018.

Yu, T., Yin, H., and Zhu, Z. Spatio-temporal graph convolutional neural network: A deep learning framework for traffic forecasting. *International Joint Conference on Artificial Intelligence*, 2017.

Zachary, W. W. An information flow model for conflict and fission in small groups. *Journal of anthropological research*, 33(4):452–473, 1977.

Zhang, B., Gai, J., Du, Y., Ye, Q., He, D., and Wang, L. Beyond weisfeiler-lehman: A quantitative framework for gnn expressiveness. In *International Conference on Learning Representations (ICRL)*, 2024.

Zhang, B., Fan, C., Liu, S., Huang, K., Zhao, X., Huang, J., and Liu, Z. The expressive power of graph neural networks: A survey. *IEEE Transactions on Knowledge and Data Engineering*, 2025.

Zhao, L. and Akoglu, L. Pairnorm: Tackling oversmoothing in gnns. In *International Conference on Learning Representations (ICRL)*, 2020.

Zhao, T., Liu, Y., Kolodner, M., Montemayor, K., Ghazizadeh, E., Batra, A., Fan, Z., Gao, X., Guo, X., Ren, J., Park, S., Yu, P., Yu, J., Vij, S., and Shah, N. GiGL: Large-scale graph neural networks at Snapchat. In *ACM SIGKDD Conference on Knowledge Discovery and Data Mining*, 2025.

A. Over-Smoothing Measures

In the literature, several measures for over-smoothing have been proposed. In our experiments, we compute all of these measures to ensure that our conclusions are drawn from a comprehensive analysis.

Most prominently, the discrete Dirichlet energy is used to quantify converging node representations. For a feature matrix with a single feature or hidden dimension $\mathbf{x} \in \mathbb{R}^{|\mathcal{V}| \times 1}$, its vectorised form is defined as

$$E(\mathbf{x}) = \mathbf{x}^T \mathbf{L} \mathbf{x} = \frac{1}{2} \sum_{i=1}^{|\mathcal{V}|} \sum_{j=1}^{|\mathcal{V}|} a_{ij} (x_i - x_j)^2,$$

where \mathbf{L} denotes the Laplacian matrix of the graph. In multidimensional space, the Dirichlet energy is defined for a continuous function $u(\cdot)$ using the Euclidean norm over all dimensions $f \in F$ by

$$E(u) = \frac{1}{2} \int_{\Omega} \|\nabla u\|^2 dx.$$

In our case, this corresponds to summing the Dirichlet energy over all feature dimensions, with $\|\mathbf{x}_i - \mathbf{x}_j\|_2^2 = (x_{if} - x_{jf})^2 + \dots + (x_{iF} - x_{jF})^2$. Since we compare the Dirichlet energy of hidden features across models with potentially different optimal feature dimensions, we normalise by the feature dimension to ensure comparability:

$$E(\mathbf{X}) = \frac{1}{F} \mathbf{1}^T \text{diag}(\mathbf{X}^T \mathbf{L} \mathbf{X}) = \frac{1}{2F} \sum_{f=1}^F \sum_{i=1}^{|\mathcal{V}|} \sum_{j=1}^{|\mathcal{V}|} a_{ij} (x_{if} - x_{jf})^2. \quad (3)$$

Rusch et al. (2023a) define a slight variation of the Dirichlet energy for measuring over-smoothing on graphs, normalising by the number of nodes rather than by two. They also apply a square root to the Dirichlet energy. Note that both the normalisation and the square root merely rescale the values and do not affect the expected exponential decay towards zero. We therefore adopt the definition in Equation (3).

The Dirichlet energy is equal to zero if and only if all node representations are identical. However, this behaviour only arises after over-smoothing for example for GAT layers (Wu et al., 2023; Cai & Wang, 2020). For GCNs, over-smoothed representations are expected to be scaled by the node degree (Oono & Suzuki, 2019). Consequently, Cai & Wang (2020) propose a degree-normalised Dirichlet energy that converges to zero for over-smoothing in GCNs. Extending this to our multidimensional formulation yields

$$E(\mathbf{X}) = \frac{1}{F} \mathbf{1}^T \text{diag}(\mathbf{X}^T \mathbf{L} \mathbf{X}) = \frac{1}{F} \sum_{f=1}^F \sum_{i=1}^{|\mathcal{V}|} \sum_{j=1}^{|\mathcal{V}|} a_{ij} \left(\frac{x_{if}}{\sqrt{1 + d(i)}} - \frac{x_{jf}}{\sqrt{1 + d(j)}} \right)^2. \quad (4)$$

Wu et al. (2023) define a node similarity measure based on deviations from the global mean feature vector:

$$\mu(\mathbf{X}) = \left\| \mathbf{X} - \frac{\mathbf{1} \mathbf{1}^T \mathbf{X}}{|\mathcal{V}|} \right\|_F, \quad (5)$$

where $\|\cdot\|_F$ denotes the Frobenius norm. This metric also converges to zero in cases where GAT-based models exhibit over-smoothing.

Chen et al. (2019) introduce the Mean Average Distance (MAD), a smoothness metric based on the cosine similarity between pairs of nodes within a target mask. In our work, we compute only the neighbourhood smoothness, defined for a given k -hop neighbourhood as

$$\mu_{\text{MAD}}^{(k)}(\mathbf{X}) = \frac{1}{|\mathcal{E}^{(k)}|} \sum_{i=1}^{|\mathcal{V}|} \sum_{j=1}^{|\mathcal{V}|} a_{ij}^{(k)} \left(1 - \frac{\mathbf{x}_i \mathbf{x}_j}{\|\mathbf{x}_i\| \|\mathbf{x}_j\|} \right).$$

In this work, we evaluate all discussed over-smoothing measures on the hidden node embeddings after the final message passing and update step. We compute each measure for every random test initialisation, and for all nodes of the graph, not only those in the test set. In Figure 1 and in Figures 2 to 4, we report the measures theoretically appropriate for the respective model type: the degree-normalised Dirichlet energy from Equation (4) and MAD with $k = 3$ for models based on GCN message passing, and the Dirichlet energy from Equation (3), the node similarity measure from Equation (5), and MAD with $k = 3$ for models using GATv2 or GraphSAGE message passing.

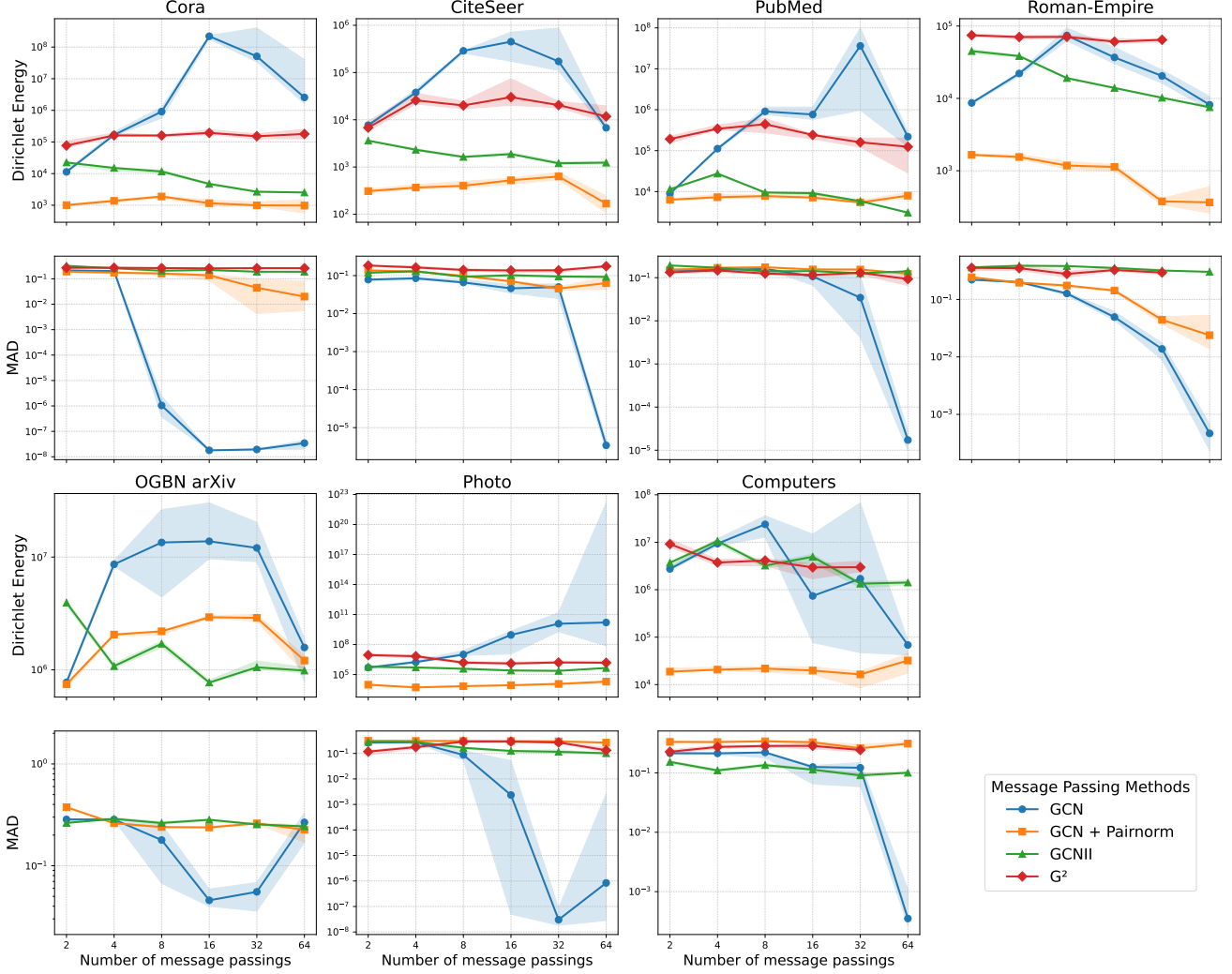


Figure 2. Dirichlet energy and MAD with a 3-hop neighbourhood of the whole dataset for all tested models with GCN message passing and datasets at different depths after hyperparameter tuning and training. The error bands represent the 25- and 75-percentiles.

B. Experimental Details

The empirical results discussed in Sections 2.3 and 3.3 were obtained through an extensive set of experiments, which will be further detailed in this appendix.

We evaluated methods against over-smoothing on seven datasets from different domains and of varying sizes. We performed experiments on the citation datasets Cora, Citeseer, and PubMed, as these are the benchmarks on which most over-smoothing mitigation methods have been developed. To further strengthen our experimental conclusions, we additionally included the citation network OGBN-arXiv (Hu et al., 2020), which is orders of magnitude larger, the heterophilic Roman-Empire text graph (Platonov et al., 2024), and the Photo and Computers co-purchase graphs from the Amazon dataset (Shchur et al.,

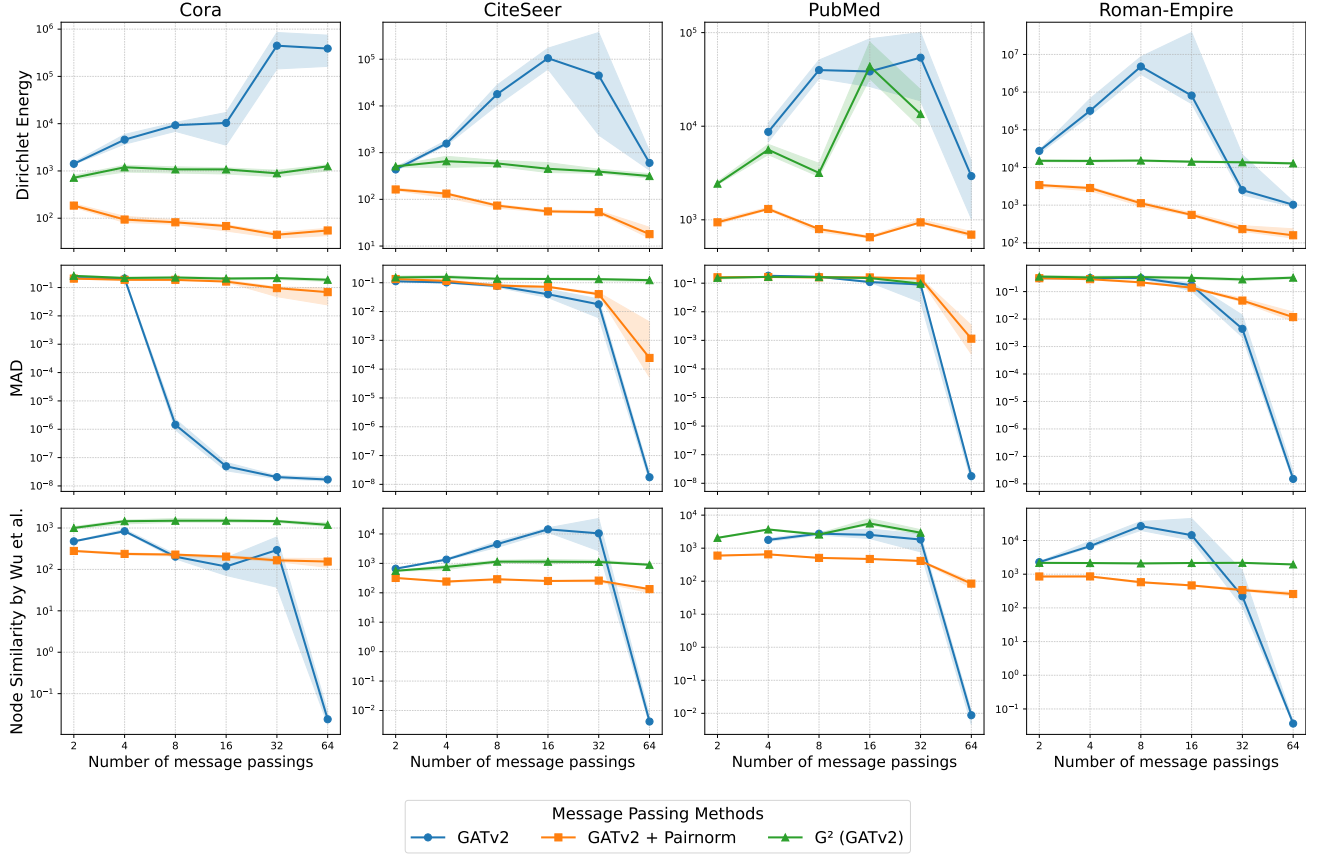


Figure 3. Dirichlet energy, MAD with a 3-hop neighbourhood and node similarity by Wu et al. (2023) of the whole dataset for all tested models with GATv2 message passing and datasets at different depths after hyperparameter tuning and training. The error bands represent the 25- and 75-percentiles.

2018). We did not include any datasets with graph-level tasks for the over-smoothing experiments, as this phenomenon has primarily been studied in the context of node-level tasks. For graph-level tasks, a performance degradation due to the convergence of node representations is also not expected, since hidden node embeddings are aggregated into a single graph representation after message passing.

For the experiments on over-squashing, we included four datasets with graph-level tasks in addition to the seven node-level datasets listed above. We used the datasets Mutag, Enzymes, and Proteins from the TU collection (Morris et al., 2020), as well as the Peptides-func dataset from the Long Range Graph Benchmark (Dwivedi et al., 2023). The former cover a range of typical domains for graph-level GNN applications, namely molecules, enzymes, and proteins. The latter dataset was chosen to validate our findings on a substantially larger benchmark.

For each model, we optimised the hyperparameters on each dataset and for each number of message passing layers $\ell \in \{2, 4, 8, 16, 32, 64\}$. The common hyperparameters, together with their search spaces or fixed values used for all models, are summarised in Table 5. In addition, Table 6 lists the hyperparameters specific to BORF and SDRF. For BORF, we defined the search spaces based on the optimal hyperparameters reported for Cora, Citeseer, PubMed, Mutag, Enzymes, and Proteins in the original paper (Yang et al., 2016). The search spaces for SDRF on Cora, Citeseer, and PubMed follow the optimal hyperparameters reported in Topping et al. (2022). For GCNII and G², the search spaces are not dataset-specific. We searched over $\alpha \in \{0.1, 0.3, 0.5\}$ and $\lambda \in \{0.5, 1.0, 1.5\}$ for GCNII, following Chen et al. (2020), and over the exponent $p \in \{1, 3, 5\}$ for G², following Rusch et al. (2023b).

The hyperparameter optimisation and testing procedures were implemented in accordance with the corresponding literature:

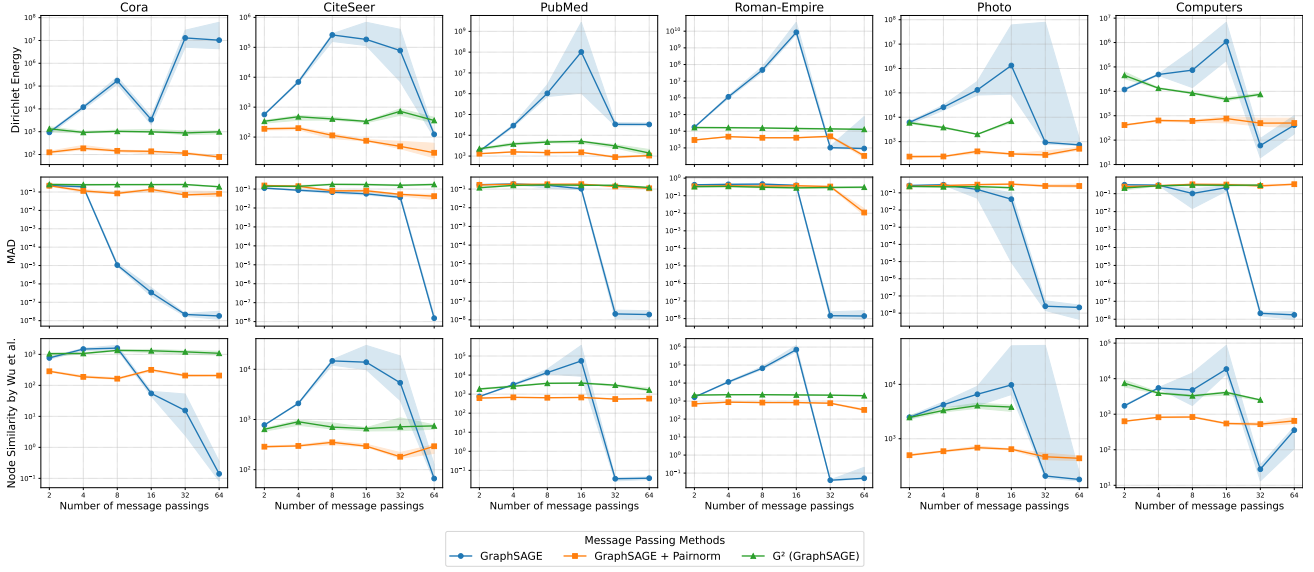


Figure 4. Dirichlet energy, MAD with a 3-hop neighbourhood and node similarity by Wu et al. (2023) of the whole dataset for all tested models with GraphSAGE message passing and datasets at different depths after hyperparameter tuning and training. The error bands represent the 25- and 75-percentiles.

- **Cora, Citeseer, and PubMed.** For the three citation networks, we used the publicly available “planetoid” split (Yang et al., 2016). For hyperparameter optimisation, we combined the train and validation sets and performed a 10-fold cross-validation. The test set remained unchanged.
- **OGBn-arXiv.** For the arXiv citation network, we used the publicly available split (Hu et al., 2020). We combined the train and validation sets and performed a 8-fold cross-validation for hyperparameter optimisation. The test set remained unchanged.
- **Roman-Empire.** For the heterophilic Roman-Empire dataset, we used the publicly available split consisting of 10 random 50%/25%/25% train/validation/test splits (Platonov et al., 2024). We adjusted the testing procedure slightly and trained and tested the model with the optimal hyperparameter setting per fold with three random parameter initialisations as suggested by Errica et al. (2020).
- **Amazon.** For the Amazon Photo and Computers datasets, we applied the 20/30/rest split described in Shchur et al. (2018). Since the original splits are not publicly available, we implemented the sampling strategy, selecting 20 and 30 samples per class for the train and validation sets, respectively. For hyperparameter optimisation, we resampled eight stratified folds from the union of train and validation sets and conducted cross-validation. The test set from the original 20/30/rest split was kept fixed.
- **Mutag, Enzymes, and Proteins.** For the three TU datasets (Morris et al., 2020), originally published by Ivanov et al. (2019), we used the publicly available 80%/10%/10% train/validation/test splits. For both hyperparameter optimisation and testing, we followed the protocol of Errica et al. (2020).
- **Peptides-func.** For the Peptides-func dataset from the Long Range Graph Benchmark (Dwivedi et al., 2023), we used the publicly available 70%/15%/15% train/validation/test splits. For hyperparameter optimisation, we combined the train and validation sets and performed a 8-fold cross-validation. The test set remained unchanged.

For the datasets for which we did not apply the Errica protocol, we evaluated each model on the test set using the hyperparameter configuration that achieved the best mean validation loss across all folds, and we report the mean over 10 random parameter initialisations.

Table 5. Search space or fixed values for standard hyperparameters defined for each dataset applied to every model; $\text{RoP}(p, lr, f, lr_{min})$ denotes a starting learning rate lr to be reduced by factor f when the validation loss plateaus with patients p down to a minimum of lr_{min} .

Dataset	Hidden size	Dropout	Learning Rate	Epochs (max)	Patience	Batch size
Cora	{32, 64, 128}	{0.2, 0.4, 0.6, 0.8}	0.001	500	30	1
Citeseer	{32, 64, 128}	{0.2, 0.4, 0.6, 0.8}	0.001	500	30	1
Pubmed	{32, 64, 128}	{0.2, 0.4, 0.6, 0.8}	0.001	500	30	1
Roman-Empire	{32, 64, 128}	{0.2, 0.4, 0.6, 0.8}	0.001	500	30	1
OGBn-arXiv	{128, 256, 512}	{0.0, 0.2, 0.4}	$\text{RoP}(25, 0.003, 0.5, 7.4e-4)$	2000	50	1
Photo	{256, 512, 1024}	{0.0, 0.1, 0.2, 0.4}	$\text{RoP}(10, 0.001, 0.5, 2.4e-4)$	3000	20	1
Computers	{256, 512, 1024}	{0.0, 0.1, 0.2, 0.4}	$\text{RoP}(10, 0.001, 0.5, 2.4e-4)$	3000	20	1
Mutag	{32, 64, 128}	{0.2, 0.4, 0.6, 0.8}	0.01	2000	500	64
Enzymes	{32, 64, 128}	{0.2, 0.4, 0.6, 0.8}	$\text{RoP}(5, 0.001, 0.5, 1e-6)$	500	50	64
Proteins	{32, 64, 128}	{0.2, 0.4, 0.6, 0.8}	$\text{RoP}(5, 0.001, 0.5, 1e-6)$	500	50	64
Peptides-func	{128, 256, 512}	{0.0, 0.1, 0.2}	$\text{RoP}(5, 0.003, 0.5, 1e-5)$	500	20	256

Table 6. Search space or fixed values for hyperparameters of preprocessing techniques for mitigating of over-squashing defined for each dataset applied to every model.

Dataset	BORF			SDRF		
	Iterations N	Edges added h	Edges removed k	Iterations N	Temperature τ	
Cora	{2, 3}	{10, 20}	{10, 20}	{100, 150}	{10, 100}	
Citeseer	{2, 3}	{10, 20}	{10, 20}	{100, 150}	{10, 100}	
Pubmed	{2, 3}	{10, 20}	{10, 20}	{100, 150}	{10, 100}	
Roman-Empire	{2, 3}	{10, 20}	{10, 20}	{100, 150}	{10, 100}	
Photo	{2, 3}	{50, 100}	{50, 100}	{100, 150}	{10, 100}	
Computers	-	-	-	{100, 150}	{10, 100}	
Mutag	{1, 2}	{3, 4}	{1, 2}	{10, 15}	{10, 100}	
Enzymes	{1, 2}	{3, 4}	{1, 2}	{10, 15}	{10, 100}	
Proteins	{1, 2}	{3, 4}	{1, 2}	{10, 15}	{10, 100}	
Peptides-func	2	12	4	25	100	

C. Extended Report of Experimental Results

In Tables 7 to 9 we report the results for all experiments, including additionally GATv2 and GraphSAGE as message passing methods.

D. Curvature Results

We investigate the impact of reducing negative graph curvature on predictive performance using a linear regression.

We evaluate the two most common graph curvature measures, namely Ollivier–Ricci curvature (Nguyen et al., 2023) and Balanced Forman curvature (Topping et al., 2022), for all graph modifications used in our experiments. These include the original graph, the expander graph employed in the EGP model, as well as the graphs rewired using BORF (Nguyen et al., 2023) and SDRF (Topping et al., 2022), in all variations arising from the possible combinations of hyperparameters, which we report in Appendix B. As BORF and SDRF aim to modify only a small number of edges, the total graph curvature does not change substantially through rewiring. Therefore, after evaluating the curvature on all edges, we sort them in descending order by curvature and compute the mean of the top n edges, i.e., the most severe bottleneck edges, where n denotes the maximum number of edges edited by either rewiring method.

For the correlation analysis, we associated each best-performing model on each dataset across all numbers of layers, that is, the scores underlined in Tables 2, 3, 8 and 9, with the corresponding graph curvature for the method and hyperparameter

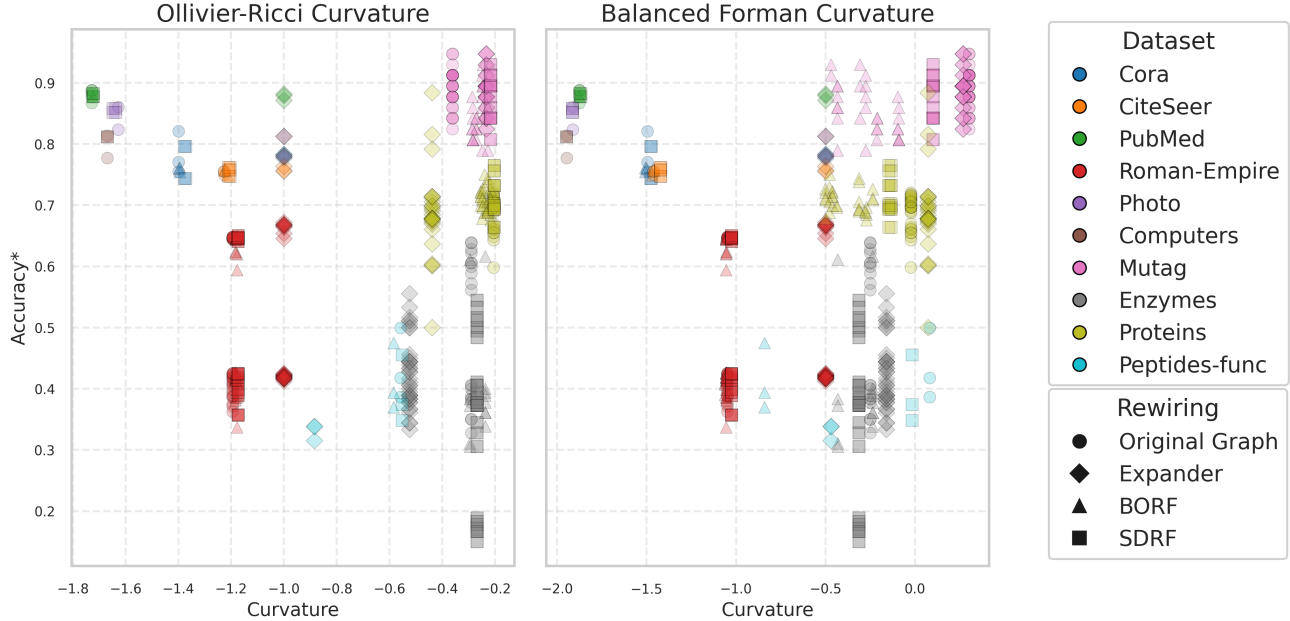


Figure 5. Accuracy (*or average precision) results for rewiring techniques to mitigate over-squashing with corresponding curvature values for the resulting message passing graph.

configuration used to obtain the result. The resulting data points are visualised in Figure 5. Note that for the datasets Roman-Empire, Mutag, Enzymes, and Proteins, we obtain ten times as many data points per method, as these models are evaluated under the Errica protocol (Errica et al., 2020), which allows the hyperparameters to vary across random initialisations and therefore results in different curvature values for each test evaluation.

From Figure 5, we do not observe any apparent correlation between curvature and accuracy. To investigate this hypothesis quantitatively, we fit a linear regression for each dataset and rewiring method, with curvature as the independent variable and predictive performance as the dependent variable. This allows us to assess the impact of curvature on accuracy via the regression coefficient of the slope. To test whether this coefficient significantly differs from 0, we apply a standard t -test. The results of these regressions are reported in Table 4.

Table 7. Full table of experiments on node-level tasks with all tested models, comprising GCN and GATv2 and GraphSAGE in combination with tested mitigation techniques for over-smoothing for a range of model depths. The accuracy is given in % with the standard deviation in brackets. The best performing model is highlighted in bold.

Dataset	Model	Layers					
		2	4	8	16	32	64
Cora	GCN	77.1 (3.3)	74.3 (0.4)	36.0 (12.4)	31.9 (0.0)	31.9 (0.0)	31.9 (0.0)
	GCN + Pairnorm	69.6 (5.5)	63.9 (5.5)	60.4 (4.7)	43.0 (9.1)	36.4 (5.5)	38.5 (9.1)
	GCNII	76.3 (2.3)	75.3 (0.3)	75.7 (0.5)	75.6 (0.2)	67.3 (17.7)	76.3 (0.4)
	G^2	74.0 (2.4)	75.2 (0.4)	74.2 (0.4)	75.0 (0.4)	75.6 (1.1)	72.8 (4.0)
	GATv2	75.5 (2.8)	73.9 (0.8)	31.9 (0.0)	31.9 (0.0)	31.9 (0.0)	31.9 (0.0)
	GATv2 + Pairnorm	69.7 (1.5)	61.5 (2.8)	63.6 (6.4)	61.8 (11.4)	40.1 (8.0)	38.8 (7.4)
	G^2 (GATv2)	76.4 (1.7)	77.7 (5.3)	76.9 (3.3)	75.0 (3.3)	76.5 (4.1)	78.5 (6.0)
	GraphSAGE	82.1 (5.1)	74.3 (0.5)	31.9 (0.0)	31.9 (0.0)	31.9 (0.0)	31.9 (0.0)
	GraphSAGE + Pairnorm	73.5 (4.9)	43.9 (6.4)	37.9 (8.1)	42.0 (3.5)	36.2 (5.2)	37.9 (5.1)
CiteSeer	G^2 (GraphSAGE)	75.2 (0.5)	75.2 (1.9)	76.6 (2.1)	77.9 (2.5)	76.2 (1.7)	78.6 (5.0)
	GCN	75.5 (0.8)	74.5 (0.7)	73.5 (0.4)	58.1 (12.3)	53.6 (19.2)	18.1 (0.0)
	GCN + Pairnorm	68.2 (1.1)	68.3 (1.6)	66.4 (4.2)	63.6 (5.2)	51.6 (5.8)	21.9 (5.3)
	GCNII	76.0 (0.7)	76.4 (0.6)	76.6 (0.6)	77.4 (0.4)	77.4 (0.4)	77.6 (0.2)
	G^2	75.9 (0.5)	76.5 (0.4)	76.1 (0.4)	74.8 (3.5)	75.7 (0.5)	76.1 (0.5)
	GATv2	75.0 (0.6)	74.1 (0.8)	72.9 (0.6)	58.7 (11.5)	39.9 (8.4)	21.1 (2.4)
	GATv2 + Pairnorm	68.4 (0.8)	66.5 (2.8)	64.6 (4.9)	63.6 (5.0)	54.0 (5.5)	21.1 (2.2)
	G^2 (GATv2)	75.5 (3.6)	76.3 (0.7)	76.0 (0.7)	75.9 (0.5)	76.3 (0.5)	75.5 (0.5)
	GraphSAGE	75.5 (0.4)	74.1 (0.4)	72.8 (0.6)	66.2 (4.7)	49.9 (16.3)	18.8 (0.0)
PubMed	GraphSAGE + Pairnorm	70.2 (1.0)	65.9 (4.8)	56.3 (10.0)	60.2 (7.3)	34.5 (6.4)	25.3 (7.8)
	G^2 (GraphSAGE)	76.8 (0.3)	76.4 (0.5)	76.2 (0.3)	76.4 (0.5)	76.6 (0.2)	76.5 (0.5)
	GCN	87.7 (0.4)	86.1 (0.2)	83.0 (4.2)	79.3 (5.6)	63.2 (11.8)	40.5 (0.4)
	GCN + Pairnorm	87.9 (0.4)	86.4 (0.3)	85.8 (0.5)	84.7 (0.3)	84.7 (0.6)	80.2 (3.0)
	GCNII	88.3 (0.3)	88.2 (0.4)	88.4 (0.2)	88.5 (0.2)	88.2 (0.2)	88.6 (0.2)
	G^2	87.6 (1.1)	87.0 (1.5)	86.8 (2.9)	80.3 (20.9)	80.2 (20.8)	63.2 (28.6)
	GATv2	OOM	86.7 (0.8)	84.7 (0.3)	73.6 (2.0)	63.1 (14.7)	40.7 (0.0)
	GATv2 + Pairnorm	87.2 (0.5)	86.8 (0.5)	84.7 (0.4)	84.4 (0.4)	82.3 (3.5)	40.9 (0.5)
	G^2 (GATv2)	88.2 (0.3)	86.6 (1.1)	79.6 (20.6)	71.6 (18.4)	73.4 (20.7)	OOM
Roman-Empire	GraphSAGE	88.3 (0.4)	88.6 (0.4)	81.4 (5.8)	75.2 (3.8)	40.7 (0.0)	40.8 (0.2)
	GraphSAGE + Pairnorm	89.0 (0.3)	89.6 (0.6)	89.2 (2.1)	88.8 (0.3)	80.7 (4.8)	72.3 (3.1)
	G^2 (GraphSAGE)	88.0 (0.3)	87.7 (0.3)	86.9 (0.3)	86.6 (1.5)	86.4 (1.0)	74.9 (23.4)
	GCN	41.5 (0.7)	27.3 (1.2)	18.7 (0.6)	16.5 (0.3)	15.0 (0.9)	14.6 (0.6)
	GCN + Pairnorm	37.3 (0.4)	20.4 (0.7)	19.6 (1.1)	20.1 (1.2)	15.5 (0.8)	17.4 (3.3)
	GCNII	56.9 (1.0)	65.1 (0.6)	61.0 (0.9)	60.3 (0.2)	59.0 (0.2)	58.0 (0.5)
	G^2	62.5 (3.3)	62.9 (2.9)	60.6 (2.3)	61.2 (3.3)	61.0 (3.0)	OOM
	GATv2	39.2 (2.1)	38.5 (2.8)	34.4 (3.7)	19.3 (3.5)	14.2 (0.3)	13.9 (0.1)
	GATv2 + Pairnorm	52.5 (2.9)	33.6 (4.0)	20.2 (1.6)	18.0 (1.0)	14.9 (0.4)	14.1 (0.4)
OGBN arXiv	G^2 (GATv2)	62.0 (3.6)	63.2 (2.2)	61.8 (3.3)	61.9 (2.4)	61.1 (3.4)	60.8 (2.4)
	GraphSAGE	64.6 (0.3)	61.5 (2.6)	46.5 (3.6)	33.2 (3.1)	13.9 (0.1)	13.9 (0.1)
	GraphSAGE + Pairnorm	66.1 (0.6)	65.6 (0.4)	66.6 (0.5)	62.3 (1.5)	35.8 (2.7)	14.1 (0.4)
	G^2 (GraphSAGE)	62.7 (3.4)	62.4 (2.3)	60.2 (4.0)	61.4 (3.5)	61.7 (3.0)	60.9 (3.0)
	GCN	55.7 (0.2)	54.2 (0.5)	32.1 (18.5)	12.2 (9.0)	7.2 (0.3)	7.0 (0.8)
	GCN + Pairnorm	60.2 (0.3)	60.3 (0.3)	61.0 (0.2)	59.1 (0.3)	53.2 (2.8)	11.8 (4.7)
	GCNII	58.2 (0.5)	58.5 (0.6)	56.4 (2.5)	56.9 (0.3)	56.6 (0.4)	56.2 (0.2)
	GATv2 + Pairnorm	60.2 (0.1)	59.4 (0.1)	59.2 (0.1)	56.7 (0.4)	OOM	OOM
	GraphSAGE + Pairnorm	60.6 (0.1)	60.6 (0.2)	60.7 (0.2)	58.1 (0.7)	30.2 (11.9)	15.8 (7.7)
Photo	GCN	86.0 (4.5)	73.7 (8.8)	48.6 (10.0)	29.9 (12.1)	22.8 (4.4)	25.9 (2.0)
	GCN + Pairnorm	87.0 (1.1)	78.0 (2.2)	81.7 (2.2)	81.4 (2.0)	78.7 (5.3)	65.0 (6.2)
	GCNII	86.9 (2.0)	86.5 (1.7)	85.5 (3.1)	84.5 (4.5)	85.0 (3.8)	85.1 (5.1)
	G^2	78.3 (6.2)	77.4 (10.7)	82.9 (3.3)	83.6 (3.2)	82.3 (3.3)	77.2 (4.0)
	GraphSAGE	82.4 (3.9)	80.5 (3.4)	54.9 (16.0)	38.7 (13.7)	24.0 (4.3)	24.0 (4.3)
	GraphSAGE + Pairnorm	75.8 (3.1)	58.5 (5.4)	69.3 (12.6)	74.7 (3.4)	51.9 (12.7)	52.2 (19.1)
	G^2 (GraphSAGE)	80.5 (6.2)	83.7 (6.0)	82.5 (5.9)	80.2 (9.4)	OOM	OOM
	GCN	77.7 (3.7)	73.1 (4.5)	54.4 (16.3)	21.1 (14.7)	24.4 (16.8)	10.7 (12.0)
	GCN + Pairnorm	80.7 (2.4)	75.3 (3.2)	76.0 (2.3)	65.3 (17.8)	45.5 (20.0)	59.2 (11.1)
Computers	GCNII	81.5 (1.9)	81.3 (1.5)	81.2 (1.7)	75.1 (14.5)	80.2 (3.9)	81.2 (2.1)
	G^2	66.1 (9.9)	74.6 (4.9)	73.3 (5.9)	70.6 (9.8)	74.5 (3.7)	OOM
	GraphSAGE	81.4 (1.7)	77.4 (4.1)	30.4 (20.6)	32.1 (15.3)	9.9 (5.5)	7.3 (4.8)
	GraphSAGE + Pairnorm	80.7 (2.3)	81.4 (2.1)	74.8 (6.1)	56.5 (21.5)	38.2 (19.4)	42.1 (14.6)
	G^2 (GraphSAGE)	73.6 (6.3)	70.3 (8.1)	75.0 (3.8)	73.2 (9.4)	67.3 (14.5)	OOM

Table 8. Full table of experiments on graph-level tasks with all tested models, comprising GIN and GATv2 and GraphSAGE in combination with tested mitigation techniques for over-squashing for a range of model depths. The accuracy (*) or average precision is given in % with the standard deviation in brackets. The best performing model is highlighted in bold. The optimal depth per model and dataset is underlined.

Dataset	Model	Layers					
		2	4	8	16	32	64
Mutag	GIN	87.7 (3.1)	86.3 (3.3)	84.2 (2.2)	86.7 (3.0)	84.4 (3.9)	88.2 (3.7)
	EGP (GIN)	91.1 (1.4)	74.6 (11.2)	61.1 (8.0)	65.8 (2.3)	63.9 (6.1)	66.0 (3.5)
	GIN + BORF	<u>88.1 (2.7)</u>	86.5 (2.0)	86.1 (1.7)	87.0 (3.9)	83.2 (4.9)	83.5 (5.2)
	GIN + SDRF	<u>89.5 (2.6)</u>	86.3 (3.0)	81.9 (3.0)	82.3 (7.3)	88.1 (3.9)	86.5 (3.8)
	GATv2	88.1 (1.0)	<u>89.6 (3.5)</u>	<u>90.4 (4.3)</u>	76.8 (14.9)	63.7 (12.4)	48.8 (13.9)
	EGP (GATv2)	83.7 (3.4)	<u>86.8 (3.9)</u>	66.0 (8.6)	57.0 (12.0)	56.5 (13.4)	63.5 (5.2)
	GATv2 + BORF	70.7 (6.5)	<u>82.8 (3.3)</u>	80.4 (5.0)	73.0 (11.2)	68.8 (12.3)	63.5 (5.2)
	GATv2 + SDRF	75.3 (6.3)	<u>87.2 (2.7)</u>	80.4 (6.8)	77.2 (8.0)	65.3 (18.2)	69.5 (9.3)
	GraphSAGE	87.0 (1.4)	<u>88.9 (1.5)</u>	87.0 (3.8)	80.5 (8.2)	63.2 (7.9)	68.4 (0.0)
	EGP (GraphSAGE)	88.2 (1.0)	<u>88.6 (1.2)</u>	78.9 (4.8)	68.4 (5.1)	54.2 (10.4)	48.6 (16.4)
Enzymes	GraphSAGE + BORF	85.4 (2.0)	<u>85.6 (2.4)</u>	81.6 (6.7)	73.0 (8.7)	65.8 (9.5)	68.2 (0.7)
	GraphSAGE + SDRF	88.1 (3.0)	86.0 (2.9)	85.3 (6.1)	80.9 (6.7)	72.8 (5.6)	72.8 (2.2)
	GIN	60.6 (3.4)	59.0 (1.4)	56.8 (3.2)	47.7 (4.3)	31.0 (3.6)	17.7 (2.5)
	EGP (GIN)	<u>50.2 (2.7)</u>	45.3 (3.8)	24.7 (3.5)	18.8 (4.4)	17.9 (3.3)	16.6 (0.4)
	GIN + BORF	<u>56.9 (2.4)</u>	<u>58.4 (2.1)</u>	57.6 (2.0)	47.1 (3.0)	30.5 (3.7)	19.1 (2.9)
	GIN + SDRF	<u>50.3 (2.6)</u>	48.4 (2.3)	44.6 (2.7)	35.9 (3.0)	27.0 (3.1)	16.4 (1.8)
	GATv2	36.3 (2.8)	<u>37.7 (2.8)</u>	30.9 (2.6)	23.3 (3.0)	16.7 (0.4)	16.7 (0.0)
	EGP (GATv2)	33.1 (3.1)	<u>38.5 (2.2)</u>	27.6 (3.6)	16.6 (2.5)	17.0 (0.6)	16.7 (0.1)
	GATv2 + BORF	<u>37.4 (4.1)</u>	33.5 (2.1)	31.3 (2.9)	24.1 (2.8)	17.1 (0.8)	16.7 (0.0)
	GATv2 + SDRF	<u>33.7 (2.7)</u>	<u>35.3 (3.1)</u>	30.4 (3.5)	23.5 (3.3)	18.1 (2.6)	16.7 (0.0)
Proteins	EGP (GraphSAGE)	29.0 (1.8)	<u>42.7 (3.3)</u>	34.2 (2.8)	22.3 (2.8)	17.4 (1.1)	16.8 (0.2)
	GraphSAGE + BORF	28.6 (1.6)	<u>31.0 (2.5)</u>	30.3 (2.8)	25.6 (3.0)	16.7 (0.0)	16.7 (0.0)
	GraphSAGE + SDRF	36.4 (1.8)	<u>38.7 (2.2)</u>	32.9 (3.4)	23.3 (3.4)	18.5 (1.7)	16.7 (0.0)
	GIN	64.0 (1.1)	64.3 (1.3)	64.2 (1.3)	63.9 (1.2)	<u>66.5 (2.2)</u>	66.1 (1.9)
	EGP (GIN)	61.8 (0.7)	65.6 (2.2)	65.7 (3.4)	<u>68.1 (8.6)</u>	<u>41.0 (15.5)</u>	46.8 (18.2)
	GIN + BORF	65.3 (1.2)	63.7 (1.0)	<u>72.6 (1.9)</u>	65.6 (2.1)	66.9 (2.1)	68.0 (1.4)
	GIN + SDRF	70.3 (0.9)	72.0 (1.3)	72.9 (1.8)	72.8 (2.0)	71.4 (2.0)	68.1 (1.9)
	GATv2	66.9 (0.7)	67.7 (0.6)	<u>69.9 (0.7)</u>	66.8 (1.5)	59.7 (5.5)	57.2 (2.8)
	EGP (GATv2)	65.4 (1.9)	<u>70.1 (1.9)</u>	<u>66.9 (4.5)</u>	59.6 (10.7)	58.5 (1.8)	59.8 (0.0)
	GATv2 + BORF	67.2 (0.5)	67.3 (0.8)	<u>69.4 (1.5)</u>	62.1 (7.7)	52.3 (7.4)	48.0 (4.6)
Peptides-func	GATv2 + SDRF	66.6 (0.5)	68.3 (0.3)	<u>69.8 (0.7)</u>	66.7 (5.0)	58.6 (7.8)	57.2 (3.7)
	GraphSAGE	68.1 (0.5)	69.4 (0.6)	<u>68.5 (0.5)</u>	<u>70.1 (0.5)</u>	61.8 (2.3)	59.8 (0.0)
	EGP (GraphSAGE)	<u>67.6 (0.2)</u>	63.2 (1.4)	55.2 (3.7)	54.8 (4.7)	55.8 (5.0)	43.7 (5.7)
	GraphSAGE + BORF	67.9 (0.3)	68.5 (0.5)	<u>70.3 (0.9)</u>	68.5 (2.0)	61.1 (2.7)	59.8 (0.0)
	GraphSAGE + SDRF	67.3 (0.4)	<u>69.7 (0.6)</u>	67.1 (0.4)	66.7 (1.3)	62.2 (3.9)	59.9 (0.0)
	GIN	59.3 (0.5)	60.7 (1.0)	57.9 (1.1)	60.7 (1.1)	55.7 (1.2)	42.2 (8.5)
	EGP (GIN)	41.6 (0.3)	<u>42.9 (0.6)</u>	21.4 (3.2)	17.5 (0.2)	17.3 (0.3)	17.2 (0.4)
	GIN + BORF	59.0 (0.8)	<u>59.7 (0.6)</u>	57.9 (1.4)	55.8 (1.4)	49.7 (0.8)	47.0 (1.4)
	GIN + SDRF	<u>56.7 (0.6)</u>	55.2 (0.8)	53.1 (0.7)	53.8 (1.0)	49.8 (1.5)	40.4 (4.1)
	GATv2	<u>41.2 (2.4)</u>	46.6 (1.1)	<u>47.8 (2.7)</u>	32.0 (7.6)	17.8 (1.2)	17.4 (1.3)
Peptides-func	EGP (GATv2)	38.0 (1.3)	<u>41.6 (1.3)</u>	<u>22.2 (6.6)</u>	17.3 (0.3)	16.9 (1.0)	17.3 (0.5)
	GATv2 + BORF	43.4 (0.6)	<u>45.5 (1.8)</u>	45.5 (1.8)	30.5 (7.7)	17.6 (0.4)	17.3 (1.0)
	GATv2 + SDRF	39.9 (0.7)	41.4 (1.1)	<u>43.3 (3.0)</u>	32.0 (5.8)	17.7 (1.0)	17.6 (1.0)
	GraphSAGE	45.2 (0.2)	48.5 (0.9)	<u>51.9 (2.4)</u>	26.0 (10.2)	18.5 (1.4)	17.7 (1.2)
	EGP (GraphSAGE)	42.4 (0.3)	42.8 (0.3)	<u>41.3 (0.4)</u>	20.7 (7.6)	17.1 (0.5)	17.0 (0.7)
	GraphSAGE + BORF	47.4 (0.5)	<u>50.1 (0.8)</u>	48.1 (1.5)	38.4 (7.0)	24.6 (0.0)	24.6 (0.0)
	GraphSAGE + SDRF	44.2 (0.2)	45.8 (1.0)	<u>46.3 (1.5)</u>	40.7 (4.0)	29.0 (2.0)	26.0 (3.6)

Table 9. Full table of experiments on node-level tasks with all tested models, comprising GCN and GATv2 and GraphSAGE in combination with tested mitigation techniques for over-squashing for a range of model depths. The accuracy is given in % with the standard deviation in brackets. The best performing model is highlighted in bold. The optimal depth per model and dataset is underlined.

Dataset	Model	Layers					
		2	4	8	16	32	64
Cora	GCN	77.1 (3.3)	74.3 (0.4)	36.0 (12.4)	31.9 (0.0)	31.9 (0.0)	31.9 (0.0)
	EGP (GCN)	<u>77.7 (4.7)</u>	31.9 (0.0)	31.9 (0.0)	31.9 (0.0)	31.9 (0.0)	31.9 (0.0)
	GCN + BORF	<u>75.4 (0.3)</u>	71.3 (6.9)	35.9 (11.9)	31.9 (0.0)	31.9 (0.0)	31.9 (0.0)
	GCN + SDRF	<u>76.2 (3.0)</u>	36.1 (12.6)	34.2 (7.0)	31.9 (0.0)	31.9 (0.0)	31.9 (0.0)
	GATv2	<u>75.5 (2.8)</u>	73.9 (0.8)	31.9 (0.0)	31.9 (0.0)	31.9 (0.0)	31.9 (0.0)
	EGP (GATv2)	<u>78.3 (4.4)</u>	31.9 (0.0)	31.9 (0.0)	31.9 (0.0)	31.9 (0.0)	31.9 (0.0)
	GATv2 + BORF	<u>76.0 (3.2)</u>	74.1 (0.6)	36.0 (12.3)	31.9 (0.0)	31.9 (0.0)	31.9 (0.0)
	GATv2 + SDRF	<u>74.4 (0.5)</u>	61.7 (15.9)	35.4 (7.5)	31.9 (0.0)	31.9 (0.0)	31.9 (0.0)
	GraphSAGE	82.1 (5.1)	74.3 (0.5)	31.9 (0.0)	31.9 (0.0)	31.9 (0.0)	31.9 (0.0)
	EGP (GraphSAGE)	<u>78.0 (4.6)</u>	31.9 (0.0)	31.9 (0.0)	31.9 (0.0)	31.9 (0.0)	31.9 (0.0)
CiteSeer	GraphSAGE + BORF	<u>76.1 (0.9)</u>	71.8 (13.7)	35.1 (9.7)	31.9 (0.0)	31.9 (0.0)	31.9 (0.0)
	GraphSAGE + SDRF	<u>79.6 (5.4)</u>	71.1 (13.6)	52.0 (15.5)	31.9 (0.0)	31.9 (0.0)	31.9 (0.0)
	GCN	<u>75.5 (0.8)</u>	74.5 (0.7)	73.5 (0.4)	58.1 (12.3)	53.6 (19.2)	18.1 (0.0)
	EGP (GCN)	<u>75.7 (0.6)</u>	63.8 (4.8)	42.6 (2.0)	20.5 (4.4)	18.5 (1.5)	18.7 (2.0)
	GCN + BORF	<u>75.9 (0.5)</u>	74.5 (0.7)	73.4 (0.7)	69.7 (4.7)	57.5 (14.0)	24.3 (9.2)
	GCN + SDRF	<u>76.1 (0.6)</u>	74.8 (0.7)	73.4 (0.6)	66.4 (5.5)	52.0 (18.9)	OOM
	GATv2	<u>75.0 (0.6)</u>	74.1 (0.8)	72.9 (0.6)	58.7 (11.5)	39.9 (8.4)	21.1 (2.4)
	EGP (GATv2)	<u>75.6 (0.5)</u>	73.9 (0.8)	60.7 (10.2)	26.1 (6.3)	18.6 (1.5)	18.1 (0.0)
PubMed	GATv2 + BORF	<u>74.9 (0.5)</u>	74.4 (0.8)	73.2 (0.7)	56.4 (12.9)	44.3 (14.7)	18.6 (1.5)
	GATv2 + SDRF	<u>74.7 (0.7)</u>	74.1 (0.8)	73.0 (0.8)	58.0 (13.0)	37.3 (10.7)	18.6 (1.5)
	GraphSAGE	<u>75.5 (0.4)</u>	74.1 (0.4)	72.8 (0.6)	66.2 (4.7)	49.9 (16.3)	18.8 (0.0)
	EGP (GraphSAGE)	76.4 (0.5)	73.3 (0.9)	61.0 (7.7)	47.3 (11.3)	24.6 (5.3)	24.2 (3.0)
	GraphSAGE + BORF	<u>75.7 (0.5)</u>	73.9 (0.7)	72.4 (0.9)	62.8 (9.9)	40.2 (18.7)	18.8 (0.0)
	GraphSAGE + SDRF	<u>75.7 (0.5)</u>	73.8 (0.6)	72.4 (0.4)	67.1 (9.0)	40.2 (21.3)	19.4 (0.0)
	GCN	<u>87.7 (0.4)</u>	86.1 (0.2)	83.0 (4.2)	79.3 (5.6)	63.2 (11.8)	40.5 (0.4)
	EGP (GCN)	<u>87.1 (0.4)</u>	86.8 (0.4)	69.1 (9.5)	40.5 (0.4)	40.4 (0.2)	40.4 (0.3)
	GCN + BORF	<u>87.7 (0.4)</u>	85.9 (0.4)	84.0 (3.2)	75.9 (12.7)	68.6 (7.8)	40.4 (0.6)
	GCN + SDRF	<u>87.7 (0.3)</u>	86.0 (0.4)	85.0 (0.3)	77.9 (5.1)	47.0 (12.5)	40.6 (0.2)
Roman-Empire	GATv2	OOM	<u>86.7 (0.8)</u>	84.7 (0.3)	73.6 (2.0)	63.1 (14.7)	40.7 (0.0)
	EGP (GATv2)	<u>87.9 (0.2)</u>	87.9 (0.5)	73.8 (1.3)	40.7 (0.0)	40.7 (0.0)	40.7 (0.0)
	GATv2 + BORF	<u>87.8 (0.4)</u>	86.5 (0.5)	83.6 (3.0)	78.4 (4.6)	54.8 (14.2)	41.0 (0.3)
	GATv2 + SDRF	<u>87.6 (0.4)</u>	86.9 (0.8)	83.6 (3.3)	71.3 (10.5)	52.7 (14.4)	40.9 (0.3)
	GraphSAGE	88.3 (0.4)	88.6 (0.4)	81.4 (5.8)	75.2 (3.8)	40.7 (0.0)	40.8 (0.2)
	EGP (GraphSAGE)	88.2 (0.3)	<u>86.7 (4.1)</u>	70.2 (10.0)	53.3 (15.0)	54.4 (12.3)	54.7 (12.0)
	GraphSAGE + BORF	87.1 (0.3)	<u>88.5 (0.5)</u>	79.2 (6.9)	73.5 (16.9)	40.7 (0.0)	40.8 (0.2)
	GraphSAGE + SDRF	<u>88.2 (0.5)</u>	87.9 (0.4)	82.1 (7.0)	72.8 (0.6)	40.7 (0.0)	40.7 (0.0)
	GCN	<u>41.5 (0.7)</u>	27.3 (1.2)	18.7 (0.6)	16.5 (0.3)	15.0 (0.9)	14.6 (0.6)
	EGP (GCN)	<u>41.9 (0.2)</u>	21.9 (0.6)	14.1 (0.2)	14.3 (0.4)	14.6 (0.9)	14.7 (1.1)
OGBN arXiv	GCN + BORF	<u>40.9 (0.7)</u>	26.7 (0.7)	18.8 (0.7)	16.5 (0.3)	15.1 (0.5)	14.4 (0.6)
	GCN + SDRF	<u>41.6 (0.7)</u>	27.3 (1.1)	18.5 (0.5)	16.4 (0.3)	15.1 (0.7)	14.7 (1.2)
	GATv2	<u>39.2 (2.1)</u>	38.5 (2.8)	34.4 (3.7)	19.3 (3.5)	14.2 (0.3)	13.9 (0.1)
	GATv2 + BORF	<u>40.5 (1.5)</u>	38.2 (2.6)	35.9 (3.3)	20.9 (2.9)	14.1 (0.4)	13.9 (0.1)
	GATv2 + SDRF	<u>39.6 (1.6)</u>	37.7 (1.9)	35.3 (3.9)	20.3 (3.6)	14.1 (0.3)	13.9 (0.0)
	GraphSAGE	64.6 (0.3)	61.5 (2.6)	46.5 (3.6)	33.2 (3.1)	13.9 (0.1)	13.9 (0.1)
	EGP (GraphSAGE)	66.4 (0.4)	58.3 (3.6)	45.9 (4.0)	20.8 (6.4)	13.9 (0.0)	14.0 (0.0)
	GraphSAGE + BORF	63.4 (0.8)	61.5 (2.9)	49.4 (3.8)	29.5 (6.4)	13.9 (0.1)	13.9 (0.0)
Photo	GraphSAGE + SDRF	<u>64.6 (0.2)</u>	62.7 (1.7)	48.5 (3.1)	30.3 (6.0)	13.8 (0.2)	13.9 (0.1)
	GCN	<u>55.7 (0.2)</u>	54.2 (0.5)	32.1 (18.5)	12.2 (9.0)	7.2 (0.3)	7.0 (0.8)
	EGP (GCN)	<u>57.6 (0.3)</u>	23.8 (10.3)	6.7 (0.4)	7.8 (0.3)	7.2 (0.7)	6.9 (1.2)
	EGP (GATv2)	<u>57.1 (0.4)</u>	55.6 (1.0)	21.7 (18.0)	5.9 (0.0)	5.9 (0.0)	OOM
	EGP (GraphSAGE)	<u>57.7 (0.5)</u>	51.7 (6.1)	44.2 (8.7)	16.5 (11.0)	20.3 (1.0)	20.1 (1.4)
	GCN	<u>86.0 (4.5)</u>	73.7 (8.8)	48.6 (10.0)	29.9 (12.1)	22.8 (4.4)	25.9 (2.0)
	EGP (GCN)	<u>77.9 (13.1)</u>	56.2 (15.9)	32.1 (9.2)	24.3 (1.8)	25.1 (1.7)	27.1 (3.0)
	GCN + BORF	<u>82.0 (5.7)</u>	71.9 (14.9)	53.1 (15.4)	31.8 (8.1)	28.9 (12.0)	25.9 (1.3)
Computers	GCN + SDRF	<u>85.8 (4.1)</u>	79.1 (6.4)	53.3 (16.3)	35.1 (13.4)	29.0 (8.8)	26.0 (1.3)
	GraphSAGE	<u>82.4 (3.9)</u>	80.5 (3.4)	54.9 (16.0)	38.7 (13.7)	24.0 (4.3)	24.0 (4.3)
	EGP (GraphSAGE)	81.2 (1.0)	76.5 (5.0)	54.0 (12.7)	26.6 (5.5)	25.8 (0.4)	25.3 (0.9)
	GraphSAGE + BORF	86.6 (1.7)	73.7 (6.4)	55.9 (22.9)	35.6 (17.0)	24.6 (1.9)	23.0 (5.7)
	GraphSAGE + SDRF	<u>85.2 (1.0)</u>	74.7 (16.6)	60.5 (19.1)	30.8 (12.6)	26.1 (0.1)	24.3 (4.3)
Computers	GCN	<u>77.7 (3.7)</u>	73.1 (4.5)	54.4 (16.3)	21.1 (14.7)	24.4 (16.8)	10.7 (12.0)
	EGP (GCN)	<u>81.3 (1.6)</u>	73.5 (1.8)	11.6 (9.8)	3.3 (2.4)	3.9 (2.2)	3.9 (3.2)
	GCN + SDRF	<u>76.1 (2.6)</u>	72.4 (4.2)	64.5 (4.6)	25.4 (17.9)	26.1 (18.6)	9.6 (11.0)
	GraphSAGE	81.4 (1.7)	77.4 (4.1)	30.4 (20.6)	32.1 (15.3)	9.9 (5.5)	7.3 (4.8)
	EGP (GraphSAGE)	<u>78.0 (2.4)</u>	74.8 (3.6)	30.2 (14.5)	9.9 (9.1)	6.9 (6.5)	6.7 (3.1)
	GraphSAGE + SDRF	<u>81.2 (1.5)</u>	75.7 (4.6)	51.2 (17.5)	16.6 (16.1)	8.4 (5.5)	11.8 (10.3)